UNIVERSITÀ
DEGLI STUDI
DI PADOVA

Sede Amministrativa: Università degli Studi di Padova

Dipartimento di Scienze Biomediche Sperimentali

SCUOLA DI DOTTORATO DI RICERCA IN BIOSCIENZE
INDIRIZZO BIOLOGIA CELLULARE
CICLO XXIII

Intracellular trafficking of anthrax toxins

Direttore della Scuola: Ch.mo Prof. Giuseppe Zanotti
Supervisore: Ch.mo Prof. Cesare Montecucco
Co-supervisore: Dott.ssa Fiorella Tonello

Dottorando: Lucia Brandi

Table of contents

Abstract

Anthrax toxins are the major virulence factors secreted by *Bacillus anthracis* during anthrax pathogenesis. They are produced as three independent multi-domain proteins which associate on the cell surface and subsequently enter the cell hijacking the endocytic route. Edema factor (EF) and lethal factor (LF) are two enzymatic subunits, whose action results in the alteration of two important cellular signaling pathways. They bind to cell surface receptors via interaction with the protective antigen (PA) binding subunit. PA is also essential for EF and LF exit from the endosomal route and delivery to the cell cytoplasm, where they act on cellular targets.

Owing to their enzymatic activity in the host cells cytosol, anthrax toxins play a key role during anthrax pathogenesis, and therefore the knowledge on EF and LF intracellular trafficking is highly important.

By imaging EF and LF C-terminally fused to fluorescent proteins in single cell we report that EF and LF reach late endosomal compartments wherefrom they translocate into the cell cytosol. We also show that after cytoplasmic translocation EF and LF have different localization, with LF dispersed into the cytosol and EF associated to endosomal membranes. The interaction between EF and late endosomal membranes is also confirmed *in vitro* by Surface Plasmon Resonance. By using a domain swap approach we exclude the involvement of EF N-terminal domain in such interaction.

Given the importance of compartmentalization of cellular signaling, we point out late endosomes as the encounter platform between anthrax toxins and their targets, highlighting compartmentalization of toxin activity as a key feature in their mechanism of action.

Introduction

1. ANTHRAX

1.1 History

Anthrax is a disease affecting primarily herbivores but all mammals, including humans, are susceptible. It has been known for a very long time and it has a very special place in science. One of the first records of anthrax was probably the "burning wind of plague" that begins Homer's *Iliad*, referring to events that were supposed to have occurred about 1190 BC. The name anthrax (coal in Greek) was actually coined by Hippocrates in the 5th century, describing a disease characterized by the black color of skin lesions and blood. The Roman poet Virgilio (70-90 BC) provided one of the earliest and most detailed descriptions of an anthrax epidemic in his *Georgics*, noting that the disease could spread to humans. Anthrax remained a major cause of death for animals, all over the planet, until the end of the 19th century.

In 1958 the WHO estimated the annual incidence of human cases of anthrax worldwide to be between 20,000 and 100,000, being more common in South and Central America, Southern and Eastern Europe, Asia, Africa, the Caribbean and the Middle East. In recent years, anthrax has received much attention from both the scientific community and other sectors of society, owing to the use of anthrax as a bioterrorist weapon in 2001.

The identification of the etiological agent of anthrax holds a very special place in the history of medicine and science. Indeed, it was by studying and analyzing anthrax that at the end of 19th century Robert Koch and Louis Pasteur showed for the first time that an infectious disease could be attributed to a given microbe, founding medical microbiology. Anthrax is caused by pathogenic strains of *Bacillus anthracis*, a rod-shaped spore forming bacterium.

Robert Koch, in his historical 1876 paper, showed that "a rod-like microorganism was consistently present in blood and tissue of diseased animals; that spores developed under starvation conditions; that

these spores could transform into the rod-like bacilli under the nutrient-rich conditions; that the rod-like organisms could be cultured in pure form; and finally that the cultured material, either in the form of rod-like microorganisms or spores, caused anthrax disease in experimentally infected animals" (Koch 1876). Louis Pasteur in 1877 reinforced this notion, unequivocally showing that the transmission of the infection was caused by the bacterium itself rather than some other hypothetical component of the inoculated blood. The work on anthrax led to the formulation of the formal methodology used to confirm the causal relationship between a pathogen and its disease syndrome (Koch's Postulates)

The pathogenic properties of *B. anthracis* were first suggested by Davaine in 1863, and they are deeply studied still today. No pathogenic microorganism has been studied for such a long time. The interest on this bacterium rose from diverse motivations throughout history [8]. At the end of the 19th century many studies were performed because of the extensive damage caused to livestock by anthrax, and the work of Koch, Pasteur and their immediate followers let do an increased control of the epizootic. Later on, during the 1950s, research on *B. anthracis* accompanied the development of programs in bacteriological warfare in different countries. In the 1980s the motivation lacked any economic or military objective, *B. anthracis* was recognized as a very interesting model to study bacterial pathogenesis at molecular, cellular and tissue level. Anthrax toxins provided a good example for a mechanism of trans-membrane translocation of proteins and more generally for bacterial toxins delivery into host cells. Lately, the 2001 anthrax letters crisis has stricken public attention and an unprecedented support has been given by governments to develop research on microorganisms that could be used in bioterrorist attacks, including *B. anthracis*. The result has been a proliferation of studies that have turned *B. anthracis* into one of the most studied pathogenic bacteria. However, many issues still need to be deeply investigated.

1.2 Bacteriology

Bacillus anthracis is a Gram-positive, aerobic, facultative anaerobic, spore-forming, rod-shaped bacterium. Dormant spores are highly resistant to adverse environmental conditions including heat, ultraviolet and ionizing radiation, pressure, and chemical agents. They are able to survive for long periods in contaminated soils and thus account for the ecological cycle of the organism. In a suitable environment, spores reestablish vegetative growth. However, the bacilli are poor survivors, and it is unclear whether existence of a complete cycle, from germination to resporulation, occurs outside the host. Indeed the particular properties of *B. anthracis*, compared with those of other *Bacillus cereus*-group bacilli sharing the same ecological niche, are consistent with a life cycle that almost exclusively takes place in the mammalian host. Spores ingested by herbivores germinate within the host to produce the vegetative forms; these multiply and express their virulence factors, killing the host. Bacilli shed by the dying or dead animal will sporulate upon contact with air, completing the cycle [9].

1.3 Pathogenesis

Anthrax is primarily a disease of herbivores, but all mammals, including humans, are susceptible when they are exposed to spores and/or infected animal products. The disease is initiated by the entry of spores into the host body. In humans this can occur via a minor abrasion, ingestion of contaminated meat or inhalation of airborne spores. Depending on the route of spore entry, infection can be manifested by three general clinical syndromes: cutaneous, gastrointestinal and inhalational (pulmonary) anthrax, respectively. Each form can progress to fatal systemic anthrax. Cutaneous anthrax, the most common clinical syndrome, presents as a painless black eschar that generally resolves spontaneously, though disseminated infection occurs in a minority of patients. The lesions are always accompanied by substantial edema. This form is easily diagnosed and can be treated with a variety of antibiotics. In gastrointestinal and inhalational anthrax the illness is insidious in the first phase, with mild symptoms of gastroenteritis, slight fever, and flu-like symptoms. Early diagnosis is difficult, and the disease develops into a systemic form that becomes treatment resistant and rapidly fatal, with shock-like symptoms, sepsis, and respiratory failure.

Indeed, inhalational anthrax is the most severe form. When spores reach the lung alveoli, they are phagocytosed by macrophages and dendritic cells and subsequently taken to regional lymph nodes. In the meantime they germinate into vegetative bacilli, a phenomenon is associated with early secretion of anthrax toxins. *B. anthracis* can overcome the lymph node's filtering and enter the lymphatic and blood circulation, where it multiplies rapidly causing massive bacteremia and toxemia which have systemic effects [10]. This second phase is accompanied by major symptoms including fever, enlarged lymph nodes, pulmonary edema with acute dyspnea, and cyanosis. The time course of this second phase is so rapid that antibiotic therapy is no longer effective at this stage, and a shock type of death follows. It is believed that the shock reaction is caused mainly by the toxins released by the bacterium with the contribution of other bacterial products [9]. Even with antibiotic therapy and life support, mortality from inhalational anthrax is high (45% in the 2001 bioterrorism attacks) [10].

1.4 Virulence factors

Fully virulent strains of *B. anthracis* carry two large plasmids, pXO1 and pXO2, which are responsible for the expression of the two major virulence factors: the poly-γ-D-glutamic acid capsule and the toxin. The polysaccharidic capsule consists of a polymer of D-glutamic acid. It was shown to have antiphagocytic properties, enabling the bacteria to evade the immune system of the host and thus causing septicemia. Although the capsule is crucial for the establishment of anthrax, the symptoms associated with the disease are the result of toxin secretion which is followed by septicemia [11].

Anthrax toxin is a combination of two binary toxins, lethal toxin (LeTx) and edema toxin (EdTx). Each toxin consists of an enzymatic component, lethal factor (LF) and edema factor (EF), and a common cell-

binding component, protective antigen (PA), which transports the enzymes into the host cell cytosol. The combination of toxemia resulting from toxin expression and septicemia induced by bacterial growth is the reason for lethality of anthrax.

Extensive research in the past two decades has been seminal in our understanding of the regulation of toxin and capsule production. The expression of *B. anthracis* toxins and capsule genes is mediated by the pXO1 plasmid-encoded transcriptional activator AtxA (Anthrax toxin Activator) [12]. AtxA regulated toxin production seems to be optimal under the host-like conditions of elevated CO_2 (≥5%) and temperature (37°C). Temperature affects the synthesis of AtxA such that cells grown at 37°C contain fivefold more AtxA than cells grown at 28°C. In contrast, CO_2 does not affect AtxA levels; the mechanism of CO_2–enhanced regulation of the toxin genes through AtxA is still unclear.

2. ANTHRAX TOXINS

Anthrax toxins are the objective of intense research. The notion that bacteria could secrete a molecule involved in pathogenesis was already mentioned by Pasteur in 1877. Only in the late 1950s, Smith and colleagues isolated the tripartite anthrax toxin and characterized its nature and activitiy.

Anthrax toxin is an ensemble of three large, multidomain proteins, which are secreted by *Bacillus anthracis* as individually non-toxic monomers, and self-assemble on receptor-bearing cells into a series of toxic, hetero-oligomeric complexes. It belongs to the family of bacterial binary A-B toxins, characterized by an A moiety which acts within the cytosol of target cells and by a B moiety that binds target cells and translocates the A moiety into the cytosol. Anthrax toxins are composed of a singe B unit, namely protective antigen (PA; 83 kDa), and two alternative A subunits: lethal factor (LF; 90 kDa) and edema factor (EF; 89 kDa). PA combines with LF to form lethal toxin (LeTx) and with EF to form edema toxin (EdTx). LF is a zinc-dependent endopeptidase, which removes specifically the N-terminal tail of mitogen-activated protein kinase kinases (MKKs). EF is a calcium- and calmodulin- (CaM-) dependent adenylyl cyclase, which elevates the intracellular cAMP concentration.

Bacterial protein toxins are secreted as soluble proteins by many bacteria and induce cell damages by a wide variety of mechanisms. A common feature of binary toxins is their ability to interact with cellular membranes at some point in the intoxication process in order to reach the cell cytosol. These membranes can be the plasma membrane, which is the target of most pore forming toxins such as Staphylococcus δ-hemolysins (δ-toxins) or membranes of cellular organelles such as or Golgi apparatus and endosomes, like in the case of shiga toxin from *Shigella dysenteriae*, cholera toxin, tetanus and botulinus neurotoxins, diphteria exotoxin A from *Corynebacterium diphteriae* and anthrax toxin.

The precise role of the two toxins in anthrax pathology remains to be fully elucidated. Earlier studies suggested that anthrax toxins are responsible for death [13], but recent acquisitions indicate that their primary targets are cells of innate immunity that would otherwise impair the multiplication of the bacilli [14, 15]. EdTx and LeTx would then act on many other cell types when their concentrations increase the final stages of the disease, associated with the widespread dissemination of *B. anthracis* in the host.

The mechanism of anthrax toxin action will be described in 4 separate sections. The first section (2.1) will address anthrax toxin subunits structures, the second (2.2) will be about the molecular mechanisms of anthrax toxin binding to cells and translocation across cellular membranes. The third (2.3) section will describe toxins trafficking through the complex endocytic pathway and which membranes are involved in toxin translocation. The last section (2.4) will cover the cellular and systemic effects of toxin delivery to the cell cytosol.

2.1 Anthrax toxin structure

Protective antigen

Anthrax protective antigen (PA), so-named for its use in vaccines, is the central component of the tripartite protein toxin secreted by *B. anthracis*. PA mediates the entry of LF and EF into the host cell. It has been shown that it also translocates chimeric proteins containing PA-binding determinants, therefore it is being evaluated for use as a general protein delivery system, mainly for therapeutic purposes [16]. The crystallographic structures of both monomeric PA and heptameric PA_{63} have been determined [3, 17]. Native PA_{83} is a long protein and contains four folding domains (Fig. 1A), mostly composed of antiparallel β-sheets. Domain 1 (residues 1-258) is N-terminal and contains two calcium ions that help stabilizing the structure, and the cleavage site (RKKR) for proteases that release the N-terminal PA_{20}. The remaining part, called domain 1' (residues 168-258) forms the N-terminal of the activated PA and mediates the interaction with EF and LF. Domain 2 (residues residues 259-487) contains a large flexible loop (β2-β3) implicated in membrane insertion, resulting in the pH driven formation of a pore, which catalyzes EF and LF translocation across endosomal membranes [18, 19]. The small domain 3 (residues 488-595) is involved in self-association of PA_{63}. The C-terminal domain 4 (residues 596-735) is the receptor-binding domain and has limited contacts with domains 1, 2 and 3, which are intimately associated. It consists of an initial hairpin and helix, followed by a β-sandwich with an immunoglobulin-like fold. Recently, the crystallographic structure of PA-receptor complex has been solved and showed that the β3-β4 loop of domain 2 also contributes to the interaction with the receptors.

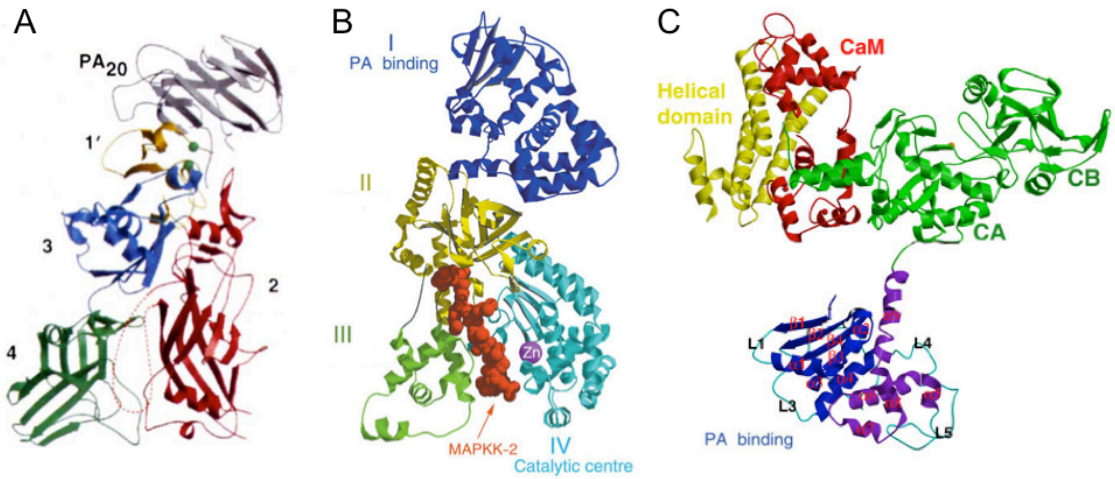

Fig.1 *Ribbon diagrams of anthrax toxin subunits*. (A) Protective antigen; (B) lethal factor. The MKK2 substrate is shown (red ball-and-stick model); (C) edema factor in complex with calmodulin (in red). [2-4]

Lethal factor

Lethal factor (LF) is a highly selective metalloprotease that site specifically cleaves proteins of the MKK family on their N-terminus region. This results in the removal of the docking sequence for the downstream cognate MAP kinase.

The crystal structure of LF (90 kDa; 776 residues) reveals that it is an elongated protein consisting of four domains (Fig. 1B) [2]. The N-terminal domain 1 (residues 1–262) comprises a four-stranded and a two-stranded β-sheets (segment 78–138) packed together with a bundle of 9-helices. This domain has a high structural similarity with the N-terminal domain 1 of EF, indicating role in binding to PA. A major part of domain 1 of LF folds very similarly to its metalloprotease domain 4, but the zinc-binding motif HExxH is replaced by YEIGK, suggesting that this domain originated from a metalloprotease domain which has been mutated during evolution in such a way as to loose its enzymatic activity and acquire PA binding properties. Accordingly, this N-terminal domain 1 of LF folds into a stable and soluble protein, termed LF_N. Mutagenesis studies indicate that some residues of domain 2 (Arg-491, Leu-514 and Asn-516) are important for the binding of the substrate MKKs in the cytosol [20], indicating that the interaction of LF with its substrate is not limited to the segment containing the cleavage site. A short LF segment (residues 303–382) folds into domain 3. This domain is a key determinant of the enzymatic activity of LF as it contributes to form with domain 4 a long cleft which is essential for the recognition and correct placement of the substrate at the active site. Domain 4 (residues 552-776) has an active site HExxH sequence that is common to metalloproteases and constitutes part of the zinc-binding and catalytic machinery [21].

Edema factor

Edema factor (EF) is a calmodulin (CaM)-activated adenylyl cyclase (AC) that increases the intracellular levels of cyclic AMP (cAMP), impairing water homeostasis and interfering with the balance of intracellular signaling pathways.

The N-terminal domain 1 (1-290) has a high structural similarity with that of LF, is centrally involved in association with PA on the surface of host cells. The C-terminal AC portion (residues 291-800) of EF shares no significant structural homology with mammalian adenylyl cyclases or any other proteins and comprises three globular domains. The active site lies at the interface of two domains, C_A (residues 294-349 and 490-622) and C_B (350-489), which together constitute the catalytic core (Fig. 1C). A third, helical domain (660-800) is connected to C_A by a linker (623-659). [22, 23]

The structure of EF bound to CaM differs significantly from that of EF, and this difference was shown to be entirely induced by CaM. CaM (16.6 kDa) is a calcium ion sensor that is expressed by all eukaryotes. Upon binding, CaM induces a conformational change which stabilizes the conformation of the substrate-binding pocket of EF, and this accounts for its high rate AC activity [22].

2.2 Anthrax toxin entry into cells

Binding to receptors

The first step of intoxication involves the binding of PA_{83} to two identified cellular receptors: ANTXR1, also known as Tumor Endothelial Marker 8 (TEM8), and ANTXR2, also known as Capillary Morphogenesis Protein 2 (CMG2) [24, 25]. These receptors are type I transmembrane proteins with a single membrane-spanning domain and they both contain an extracellular domain that in highly related to von Willebrand factor type A (VWA) domains and integrin inserted (I) domains. The two receptors share 40% overall amino acid identity and 60% identity within their VWA domains [26]. The WVA domains of TEM8 and CMG2 contain a metal ion-dependent adhesion site (MIDAS), which binds a divalent cation (i.e. Mg^{2+}, Mn^{2+}) and was demonstrated to be involved in PA binding. In fact, the mutation of a MIDAS residue (Asp 50) causes a loss of binding of TEM8 to PA [27]. The affinity of the TEM8 VWA domain for PA in the presence of different divalent cations (Kd in the μM range) is reminiscent of that seen with integrin-ligand interactions. By contrast, the affinity of PA for the VWA domain of CMG2 is approximately 1000-fold higher [28].

The cytoplasmic tails of both anthrax toxin receptors appear to have multiple roles. It was shown that TEM8 cytoplasmic region modulates PA-binding affinity presumably through its interaction with cytoplasmic factors [29]. It has been proposed that TEM8, like integrins, can exist in either a low or high affinity ligand-binding state and that the switch could occur through an inside-out signaling mechanism. The molecular details of how the cytoplasmic tail regulates the binding affinity for the TEM8 VWA domain for PA remain to be elucidated. In addition, the cytoplasmic tail is important in regulating the half-life of the proteins. It was shown that palmitoylation of cytoplasmic cysteine residues increase the half-life of proteins at the plasma membrane by preventing their premature removal from the cell surface. Moreover, TEM8 and CMG2 cytoplasmic tails are responsible for guiding and promoting the endocytosis process, in particular when triggered by anthrax toxin [30].

TEM8 and CMG2 are ubiquitously expressed [24, 25, 31]. Their physiological functions are fully elucidated, even if it was shown they are associated with binding to extracellular matrix components. Both receptors are expressed on endothelial cells during angiogenesis, whereas TEM8 is over-expressed during tumor angiogenesis and CMG2 expressed both in normal epithelial cells and in other tissues [31]. Intriguingly, EdTx action can stimulate the up-regulation of the expression of both receptor types in macrophages by a mechanism that requires the adenylate cyclase activity [32, 33], raising the possibility that EdTx can serve to amplify the effects of anthrax toxin through up-regulating receptor levels on the surfaces of susceptible cell types. It is currently unclear if *B. anthracis* has evolved to use

these two types of receptor only because they serve as efficient portals of entry into the cell or whether there are additional aspects (e.g. their associated cell-signaling pathways) of these molecules that might also be important for other aspects of anthrax pathogenesis.

Anthrax toxin has evolved to bind a receptor that does not undergo constitutive endocytosis but ligand-induced, endocytosis. This exclusion of the toxin-receptor complex from constitutive endocytosis appears to be due to S-palmitoylation of at least two cysteine residues located in the cytoplasmic tail of the two anthrax receptors. S-palmitoylation is a reversible modification that consists of the addition of C16 carbon saturated fatty acid acyl chain to cytoplasmic cysteine residues via a thioester linkage.

Formation of heptameric PA_{63} prepore

After receptor binding on the cell surface, PA_{83} is proteolitically activated by furin-like cell surface membrane proteases. The enzymatic cleavage of PA causes the removal of a 20 kDa N-terminal fragment (PA_{20}), eliminating a steric clash that prevents native PA from oligomerizing [34]. The remaining receptor bound PA_{63} self-associates to form a ring shaped heptameric complex on the cell surface called prepore [35]. The formation of the heptameric PA_{63} prepore is crucial for the toxic activity of anthrax toxins. It mediates EF and LF binding, enabling the formation of toxic complexes on the cell surface followed by their endocytosis (Fig. 2).

The crystal structure of the soluble $(PA_{63})_7$ prepore have been solved and shows a hollow ring, 85 Å high and 160 Å in diameter, with the subuints packed like pie wedges. There are no major conformational changes from the structure of monomeric PA_{83}. Domains 1' and 2 form the inside of the ring, and domains 3 and 4 are on the outside [3, 17]. A flat hydrophobic surface is exposed on domain 1' at the top of the structure and represents the binding site for LF and EF [36].

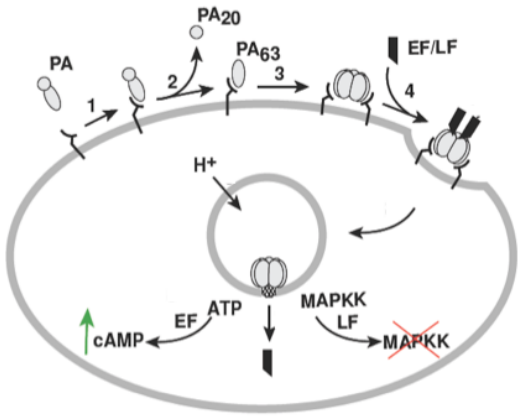

Fig. 2 *Anthrax toxin assembly and entry into host cells.* Upon binding to the receptor (1), PA is cleaved by a membrane protease (2). The remaining PA_{63} heptamerizes (3) forming $(PA_{63})_7$ prepore., which binds EF and LF (4). The assembled toxins are endocytosed and trafficked to endosomes. Acidic endosomal pH triggers a cormational change in $(PA_{63})_7$ promoting the translocation of LF and EF across the membrane. LF is a metalloprotease that cleaves members of the MAPK family EF is an adenylyl cyclase that increases the intracellular cAMP levels.

EF and LF binding

LF and EF bind to $(PA_{63})_7$ competitively via homologous N-terminal domains, termed LF_N and EF_N, respectively [37-39]. LF_N and EF_N correspond to discrete folding domains and are loosely tethered to the C-terminal, multidomain catalytic regions of these proteins. PA is able to bind LF and EF only after it has been proteolytically activated and the PA_{63} fragment has self-associated to form heptamers [36]. A high-affinity ligand (LF/EF) binding site is formed on $(PA_{63})_7$ prepore at interface between two adjacent PA_{63} subunits, and it is consistent with the results showing that heptameric $(PA_{63})_7$ prepore binds a maximum of three molecules of LF, EF or LF_N [36, 40, 41]. By directed mutagenesis it was shown that the Lys197 residues on two neighboring PA_{63} subunits can interact simultaneously with separate sites on a single LF_N molecule, thereby providing further evidence that the LF/EF binding site encompasses two adjacent subunits of the prepore. Studies on the orientation of LF_N docked to the prepore showed that helix 1 of this domain, which extends into solution from the main body of the domain, positions the highly charged and disordered N-terminal region (residues1-26 of LF) directly over the lumen of the prepore (Lacy et al., 2005)

Formation of heptameric pore

Following lipid-raft association, anthrax toxin-receptor complexes are thought to be internalized by clathrin-coated pits and thus enter the endocytic pathway [30]. Upon endosomal acidification, $(PA_{63})_7$ prepore inserts into endosomal membranes forming a pore in the bounding membrane, promoting the translocation of EF and LF across endosomal membranes, which eventually results in the delivery of the active subunits to their cellular targets in the cell cytosol.

It was shown that $(PA_{63})_7$ prepore is stable in solution at pH ≥ 8, and readily dissociates into monomers when exposed to SDS [35], but when the pH is lowered to the acidic range, the prepore undergoes a conformational rearrangement that enables it to insert into membranes, forming an ion-conductive channel in both artificial bilayers [42] and in cells [43]. The conformational transition of $(PA_{63})_7$ prepore to pore was reported to be maximal at pH 4.7 [43]. The pH dependence of pore formation by $(PA_{63})_7$ is absolutely crucial because premature pore formation on the plasma membrane would kill the host cell by altering membrane permeability and potential, as occurs in the case of pore forming toxins. This would trigger an inflammatory response, a host reaction *B. anthracis* aims to prevent.

The mechanism of pH dependent pore formation centers on the mobile loop 2β2-2β3 (residues 303–322) of domain 2. The seven 2β2-2β3 loops of the heptamer were proposed to move away from domain 2 during a pH-dependent conformational rearrangement and to interact forming a 14-strand β-barrel spanning the membrane on the base of the structure (Fig. 3A) [3, 44].

$(PA_{63})_7$ pore complex has typical properties of integral membrane proteins such as SDS-resistance and the tendency to aggregate in aqueous solutions. These features have made analysis of its structure

difficult. It has been shown that the *E. coli* chaperonin GroEL can bind PA prepore and pore inhibiting aggregation of the latter, thus providing a molecular scaffold for structural analysis, therefore the structure of PA pore was reconstructed [45]. The pore was seen to be mushroom-shaped with a ~125Å-diameter cap and ~100Å-long stem. The membrane spanning region, corresponding to the 2β2 and 2β3 loops, comprises the distal third of the stem (Fig. 3B). The turn region of the loop contains a hydrophobic tip formed by two phenylalanine residues, Phe313 and Phe314, which may aid in insertion and stabilization of the stem in membranes. The β-barrel is principally lined by residues with small side-chain volumes. A conserved phenylalanine (Phe427) in a mobile, solvent-exposed loop in the lumen plays a major role in protein translocation through the pore, which is estimated to be ~12-15 Å in diameter [1]. By modeling it has been predicted to accommodate the N-terminal residues of LF in an α-helical configuration [46]. Taken together, these observations strongly suggest proteins must unfold in order to translocate across PA channel.

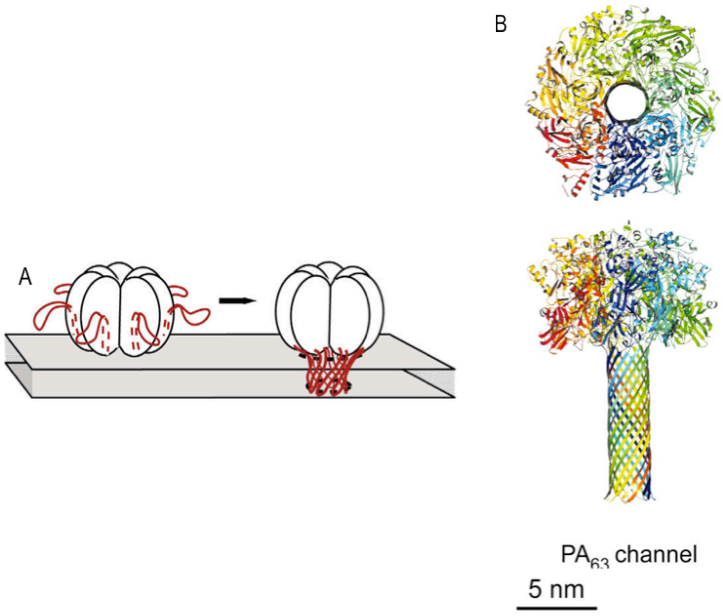

Fig. 3 *$(PA_{63})_7$ pore*
(A) Conformational transition from prepore to pore. 2β2-2β3 loop is shown in red. (B) A model of $(PA_{63})_7$ pore, each color represents a PA monomer [1].

Translocation

Structural observations on the lumen of the PA pore strongly suggest that EF and LF must unfold in order to translocate through the narrow cation selective PA channel. The acidic pH conditions of the endosomal lumen (pH 5-6) seem to facilitate unfolding of LF and EF as a prelude to their entry into the PA pore and translocation across PA pore. The pH dependence therefore ensures the coupling between PA channel formation and LF/EF translocation.

The key features underlying EF and LF translocation through PA pore have been widely studied. An electrophysiological system for studying translocation across planar lipid bilayers involving only toxin

proteins has yelded invaluable data on the process [19, 47]. However, up to now, the efficiency of the translocation of EF and LF from the endosome is not known.

The translocation of the unfolded polypeptide is initiated, under the influence of acidic pH, by the entry of the N-terminus of LF and EF into the pore, and to proceed in an N- to C- terminal direction, and the proteins eventually refold once the translocation is completed. The crystallographic structure of LF shows that the N-terminal 30 residues comprise a disordered region containing high density of charged residues. This flexible region was shown to be necessary for translocation. In fact, deleting more than ~20 residues from the N-terminus of LF_N strongly impaired acid-induced translocation of LF_N across the plasma membrane without significantly affecting its binding to PA in cultured cells [19]. There is evidence that entry of the N-terminus on LF_N into the pore depends primarily on its having a net positive charge. The disordered N-terminal regions of LF and EF are densely populated by charged residues, approximately equal numbers of positively and negatively charged residues. At acidic pH values, neutralization of the acidic residues is be expected to give the region a positive charge and cause the N-terminus to be pulled by electrostatic attraction into the negatively charged pore, perhaps aided by a positive transmembrane potential [48]. The notion that positive charge is key to initiate translocation through the PA_{63} pore is supported by the finding that fusing a 6xHis tag to the N-terminus of N-terminally truncated forms of LF_N [19] or of LF [49] increase the ability to undergo translocation across the $(PA_{63})_7$ channel.

Certain mutations in PA have given important clues to the mechanism by which the pore functions in translocation. Recent studies indicate that the pore does not serve simply as a passive channel, but rather, actively catalyzes the passage of substrate proteins across the membrane. This conclusion derives primarly from studies on the mutation of a phenylalanine residue (Phe427), lying in the 2β10-2β11 loop, which was found to strongly impair the translocation of LF_N across planar lipid bilayers [47]. In the crystallographic structure of the prepore, the Phe427 residues are seen to be luminal, near the base of the structure, and ~15-20Å apart in neighboring subunits. Evidence from paramagnetic resonance spectroscopy (EPR) measurements suggested that these residues move into close proximity (<10Å) during prepore-to-pore conversion, and they were shown to remain luminal and solvent-exposed. This structure, named phenylalanine clamp (Phe clamp), can be viewed as an active site crucial for protein translocation. It creates an environment that mimics the hydrophobic core of the unfolding protein. Transient interaction of the hydrophobic segments of the translocating polypeptide with the Phe clamp would thereby reduce the energy penalty of exposing hydrophobic side chains to the solvent or to the hydrophilic lumen of the channel. Alternatively, the Phe clamp may function in forming a seal around the translocating polypeptide, blocking the passage of ions. This seal would thus preserve the proton gradient across the membrane, and thereby maintain this gradient as a potential energy source for driving LF and EF translocation through the pore [50].

EF and LF N-terminal domain

The N-terminal domain of LF (domain 1, residues 1-262) comprises a four-stranded and a two stranded-β-sheets (segment 78-138) packed together with a bundle of 9-helices. This domain has a high structural similarly with the N-terminal domain of EF (domain 1, residues 1-290) (Fig. 4A). Indeed, LF and EF show high levels of identity (35%) and similarity (55%), principally localized in the first ~250 N-terminal residues, and similar structure [37] (Fig. 4B). EF and LF homologous N-terminal domains, termed EF_N and LF_N respectively, correspond to discrete folding domains of the parent proteins and are loosely tethered to the catalytic regions of these proteins [2, 22]. Moreover, they share crucial functions for the entry and delivery of the subunits to the cytosol.

LF_N can be fused to a variety of other proteins, such as portions of *Pseudomonas* exotoxin A (FP59) [39, 51], shiga toxin A or the enzymatic A chain of diphteria toxin (DTA) [52], which can thus bind to PA and translocate across PA channel into the cytosol. Such systems represent very efficient tools both for general protein delivery into cells, such as therapeutic agents, and for reporting LF entry into cells.

N-end rule is believed to be involved in LF toxicity. The N-end rule relates the *in vivo* half-life of proteins to the identity of their N-terminal residue. Ubiquitin ligases target protein substrates that bear specific (destabilizing) N-terminal residues, resulting in their proteasomal degradation. LFs with different N-terminal residues display different toxicities in cells and mice, and this was interpreted as LF being submitted to the N-end rule of protein degradation, so that the N-terminal residue of LF would determine the cytosolic stability and thereby the potency of LF [53, 54].

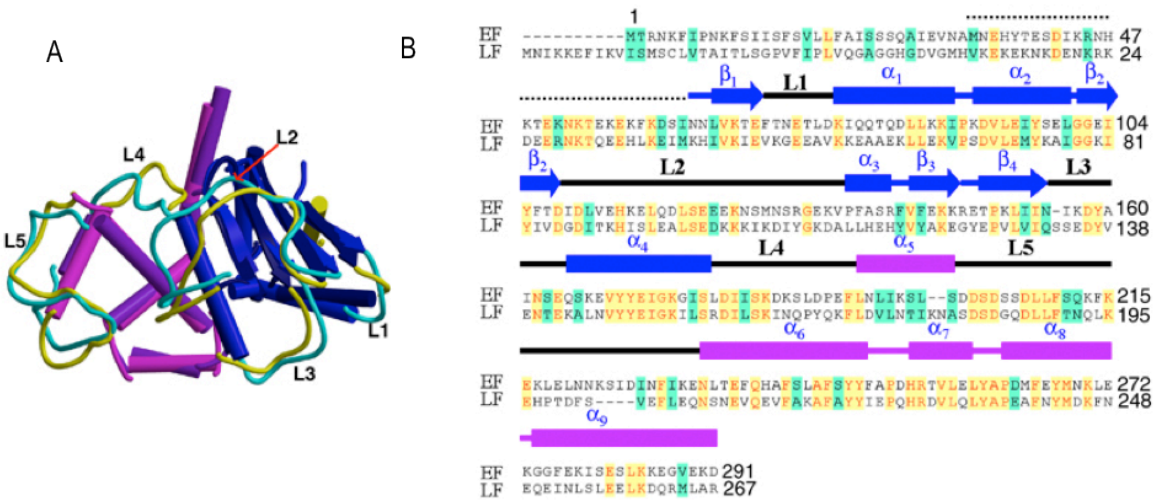

Fig. 4 *Comparison of N-terminal PA-binding domains of EF and LF.* (A) LF_N (dark blue and magenta, yellow loops) and EF_N (blue and purple, cyan loops) secondary structures. (B) sequence alignment of EF_N and LF_N. identical sequences (yellow) and similar sequences (green) are indicated [4]

2.3 Trafficking along the endocytic pathway

All bacterial A-B toxins must reach the cytoplasm of a target cell in order to exert their action. Passing through the plasma membrane, although appears as the simplest solution, turns out to be the rarest option that is used. The most frequent solution is penetrating into the cell through an existing entry mechanism (i.e. endosomal-degradation pathway) and then moving within the vesicular apparatus of the cell to finally reach the site form where the toxic action occurs. However, by using such cellular entry mechanism, pathogens and their virulence factors take the risk of getting trapped in a pathway that leads to degradation. This danger has created strong evolutionary pressure, selecting for toxins that have developed the capacity to optimally use intracellular endocytic trafficking, and this is indeed the case of anthrax toxin.

Studies focused on the molecular mechanisms involved in anthrax toxins entry and trafficking through the endocytic pathway have been extremely fruitful in the analysis endocytic organelles and the key processes that regulate such a complex pathway as endocytosis and degradation. Over the past 30 years much work has been devoted to this field and the knowledge on endo-lysosomal pathway mechanisms has enormously grown. Therefore, before addressing anthrax toxin trafficking through the endocytic pathway, an overview on endocytosis and degradation pathway is needed.

Overview of the endocytic pathway

Eukaryotic cells rely on endocytosis to internalize segments of plasma membrane, cell-surface receptors, and various soluble molecules from the extracellular environment. This pathway is composed of different organelles, known as endosomes, which communicate in a unidirectional manner from early to late endosomes to lysosomes. In addition to mediating the uptake of nutrients, endosomes are also involved in antigen presentation, signaling and receptor down-regulation from the plasma membrane. Internalized molecules can enter the cells through several routes, which can be classified in clathrin-dependent and clathrin-independent entry pathways, and their endocytosis can be triggered by ligand binding or constitutive. All endocytic routes are thought to converge into conventional endosomes, wherefrom internalized molecules can then undergo different fates, some being routed towards lysosomes for degradation, others (which will not be described in this section) being recycled back to the plasma membrane.

Endocytosed molecules and receptors are differentially sorted depending on their fate and function. Sorting occurs in at least three different stages of the endosomal pathway: the plasma membrane, the early endosomes and the late endosomes. Despite the entry site, all endocytic routes are thought to converge, directly or indirectly, into the canonical early endosomes (EEs), where sorting of the

internalized cargoes occurs. Some lipids and proteins, in particular housekeeping receptors, are recycled back to the plasma membrane, while other proteins such as receptors and ligands that need to be degraded in lysosomes, are rapidly collected within forming multivesicular bodies (MVBs). In EEs these two distinct circuits are well separated, both topologically and functionally, to ensure correct sorting. Cargoes destined to degradation are sorted from MVBs to late endosomes (LEs) and delivered to lysosomes for degradation.

Small GTPases and phsphoinositides are considered as endosomal markers for their restricted distribution (Fig. 5). However, the boundaries between two easily distinguishable compartments in the same pathway are not so well defined at the molecular level, in part because proteins that regulate membrane transport are often found in more than one compartment. For example, one of the widely used criteria to distinguish early from late endosomes is the presence of the small GTPase Rab5 on EEs and Rab7 on LEs, even though both are present on MVBs, the transport intermediates between early and late endosomes [55]. Moreover, Rab5 is also associated with the plasma membrane, where its activity seems to be related to CCVs formation [44].

Phosphoinositides that contribute to identity different endosomal organelles are transient forms of phosphatidylinositols (PI), with phosphates added by specific kinases to the positions 3, 4 or 5 on the inositol ring. Since modifying enzymes are heterogeneously localized in the cell, PIs are clustered in distinct intracellular membranes. For example, while PI3P is mainly detected on EES, $PI(3,5)P_2$ is found in LEs and Lysosomes. Conversely, they are both presenti in MVBs [56].

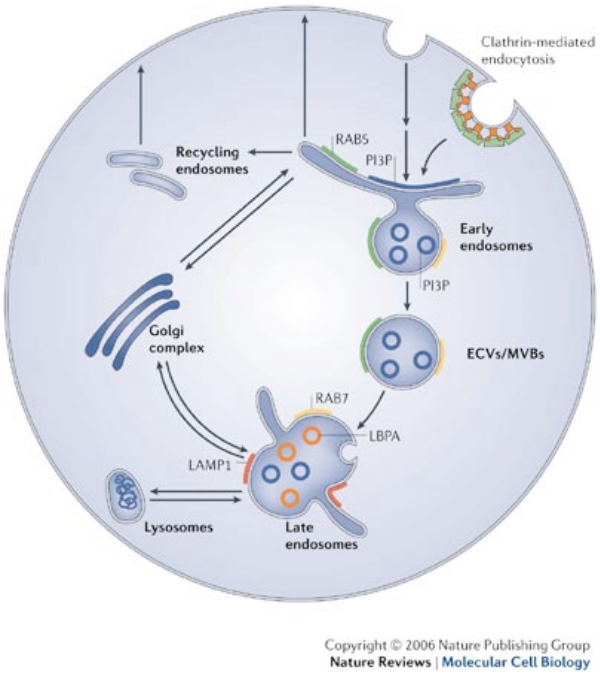

Fig. 5 Schematic view of the endocytic pathway The distribution of some important prteins and lipids in endosomal membranes is depicted [6].

Moreover, different membrane microdomains with different biophysical properties have been recently shown to coexist in each endocytic compartment. These domains consist of specialized protein-lipid combinations, or of protein complexes associated with specific membrane lipids. Whereas some of these molecular assemblies can be found in more than one compartment, a given combination seems to be unique to each compartment. The dynamic interplay between different membrane domains is thought to be responsible for the specific organization of each compartment and for the regulated trafficking of cargo molecules [57]. These findings make the endocytic pathway a highly complex and finely regulated system of vesicular trafficking.

Entry at the plasma membrane: clathrin-dependent and clathrin-independent endocytosis.

Endocytosis occurs by multiple ways of entry, which can be classified in clathrin-mediated (CME) and clathrin-independent (CIE). Clathrin-dependent endocytosis is the best-characterized mechanism for the entry of molecules (such as nutrients, receptors, growth factors, antigens and pathogens) into the cell.

The central defining feature of CCVs formation is the recruitment of soluble clathrin molecules from the cytosol to the plasma membrane. Clathrin units, called triskelions, are three-legged structures consisting of three heavy and three light chains. Clathrin main function is to form a supportive lattice around invaginating and budding vesicles. Both *in vitro* and *in vivo* clathrin triskelions are able to polymerize to form polyhedral cages or lattices at the plasma membrane, forming clathrin-coated pits (CCPs), complex structures that concentrate surface proteins for internalization. These 100-110 nm structures are observed on the plasma membrane and internal organellar surfaces, such as the trans-Golgi network (TGN).

Although clathrin forms the scaffold that is the mechanical backbone for CCPs, adaptor proteins (APs) bind to both clathrin and membrane comonents, enabling the clathrin scaffold to adhere to the membrane. APs are also required to link clathrin to the cargo carried in the vesicle. About 20 different forms of clathrin adaptors are known, among them AP1 and AP2 are the most widely recognized; AP1 is active at the TGN and AP2 at the plasma membrane. AP2 has two phophoinositide binding sites, one of which has high affinity for phosphatidylinositol-4,5-bisphosphate (PIP2), the prevalent phosphoinositide specie present at the plasma membrane. In addition, adaptors also recognize cargo proteins via direct interaction with specific amino acid sequences, either structural features or ubiquitin molecules, on the cytosolic tail of the membrane cargo protein, mediating their endocytosis and sorting to lysosomal degradation

The scission of a fully invaginated CCP to form a CCV is mediated by the large GTPase dynamin. Deeply invaginated CCPs are characterized by the presence of a neck structure that connects the forming vescicle to the plasma membrane and specifies the site of fission. The neck is constricted sufficiently to bring the opposing membrane together in order to cause fusion with the neck and the

formation of a free CCV. Dynamin self-assembles into helical collar around the neck of the CCPs and regulates the actin filaments assembly at the site of endocytosis needed to provide force to induce the scission of forming vesicles. Once fission of the vesicle has occurred, the clathrin coat is rapidly shed to enable fusion of the vesicle with its target membrane and recycle coat components for further rounds of vesicle budding.

CCVs are involved in the endocytosis of a wide variety of plasma membrane proteins and receptors such as transferrin receptor (Tf-R), low density lipoprotein-receptor (LDL-R), β_2-adrenergic receptors, CD4, insulin receptor, T- and B- cell receptors. By regulating cell surface receptor endocytosis, clathrin structures participate in endocytic regulation of cell signaling. Moreover, many pathogens exploit clathrin-dependent endocytosis to enter host cells.

Unlike clathrin-mediated endocytosis (CME), little is known about the fundamental parameters of various clathrin-independent endocytic (CIE) routes, namely Arf6 regulated, CLICC/GEEC, RhoA regulated, caveolae-dependent pathways. However, boundaries between these pathways are not always distinct and there can be regulatory interactions between different pathways. How the various CIE pathways form, why they mediate the uptake of certain types of cargo proteins, their contribution to total endocytic capacity and, importantly, what cellular roles they play remain poorly understood. Clathrin-independent pathways have been shown to be sensitive to cholesterol depletion and to inhibitors of actin polymerization but they differ in their mechanism and kinetics of formation and molecular machinery involved. Little is known about how cargo is selected for the different CIE pathways. In contrast to CME, which involves specific adaptor molecules in the cargo recruitment to CCPs, no such well-defined adaptors for CI have been found. One potential mechanism for cargo recruitment that has been considered is sorting based on the association of cargo with membrane microdomains.

Early endosomes

Early endosomes are well-defined but dynamic compartments, with high homotypic capacity, which function as the first sorting station along the endocytic pathway [57]. They have a highly complex and pleiomorphic organization that consists of cisternal regions with occasional intralumenal vesicles (ILVs), which arise from invagination and fission of EEs membrane and therefore contain cytosol, and an array of tubular subdomains where membrane cargoes destined for a range of other compartments are sorted. Molecules with different subcellular destination, such as transferrin receptor (Tnf-R), epidermal growth factor receptor (EGF-R) and cation-independent mannose-6-phosphate receptor (CI-M6PR) are all delivered to the same early endosome but it was recently shown they exit this organelle through distinct compartments [58]. However, the identification of sorting signals in the cytoplasmic domains of cargo proteins has been particularly difficult. No recycling motifs have been identified, which leads to the idea that recycling to the cell surface occurs by default. On the contrary multiple monoubiquitylation and

Lys-63 linked polyubiquitylation have been shown to function as sorting signals for protein degradation in the lysosome. Ubiquitylated proteins destined for degradation are sorted by the ESCRT machinery into ILVs and avoid recycling to the plasma membrane or retaining in the limiting endosomal membrane (Fig. 6) [7].

Growing evidence indicate that EEs represent a population both morphologically and functionally heterogeneous, whose complexity is enhanced by the presence of biochemically distinct membrane subdomains within individual organelles.

Early endosomal membranes as well as the internal membranes of MVBs mostly contain PI3P, which interacts with specific effectors containing conserved PI3P binding domain, such as the FYVE or the PX domains. Most of the FYVE- and PX- containing proteins were shown to be involved in endosomal membrane trafficking, protein sorting and signaling [6]. The presence of PI3P on early endosomal membranes is linked to the presence of Rab5 because the kinase that generates this phosphoinositide is a Rab5 effector, therefore the synthesis of PI3P is regulated by Rab5. Moreover several Rab5 effectors contain PI3P-binding FYVE domains, for example the tethering protein early endosome antigen-1 (EEA1), involved in endosome fusion and restricted to early endosomes.

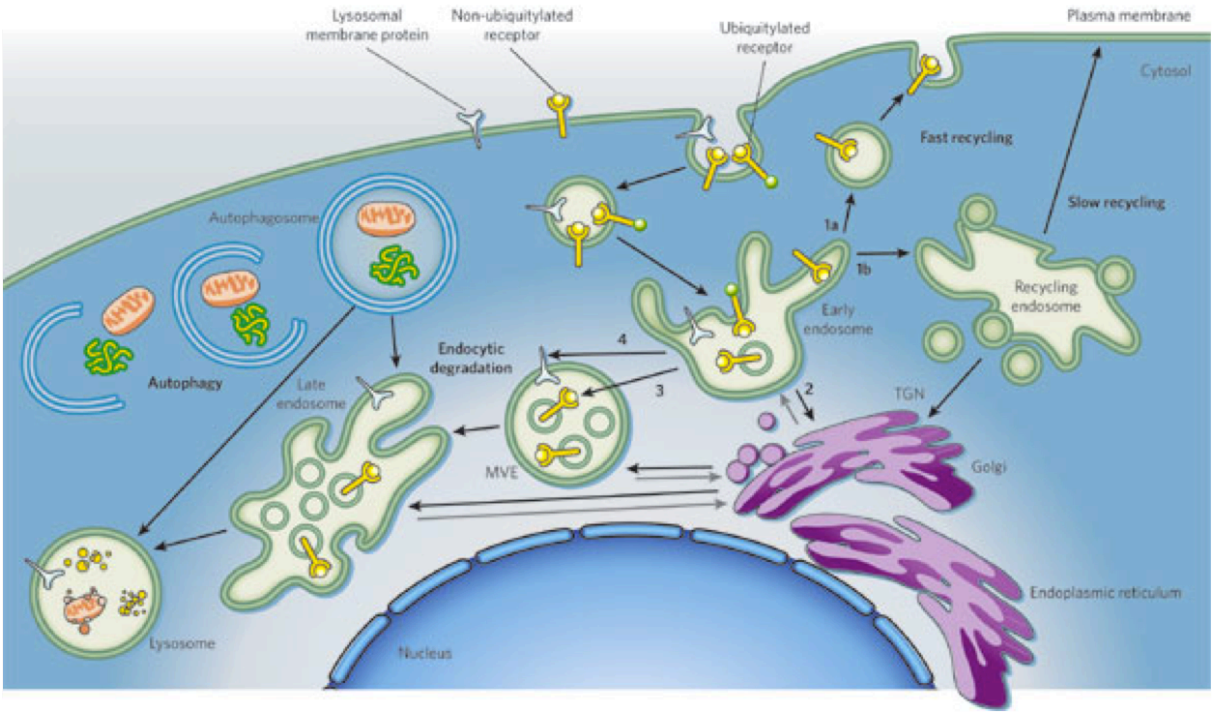

Fig. 6 *Endocytic interanlization and sorting* Different membrane proteins are sorted to distinct destinations. Some cargoes are recycled back to the plasma membrane (1). Ubiquitylated membrane proteins are sorted into ILVs and eventulally end up in the lysosomal lumen via LEs (3). In contrast, other proteins such as lysosomal membrane proteins, are sorted to the limiting membrane of the MVEs (4) [7].

Multivesicular bodies (MVBs)

Multivesicular bodies (MVBs) are large organelles (~ 400-500 nm), typically spherical, which rapidly acidify (pH ~5.5) and mediate the transport between early and late endosomes along the degradation pathway. Whether MVBs change in composition as they undergo a maturation process or whether they mediate transport between two stable compartments, is still debated. Either way, once formed, MVBs move from cell periphery towards LEs, localized in the perinuclear area, in a microtubule- and motor-dependent fashion [57].

MVBs contain two distinct membrane domains, intralumenal vesicles (ILVs) with a diameter of 40-90 nm and limiting membrane. The composition of the limiting membrane is not known except that it seems to lack the majority of early and late endosomal proteins. Similarly, little is known about ILVs membrane composition. Electron microscopy studies showed that PI3P is abundant within MVB internal membranes, in addition to EEs [59].

MVEs contain molecules that have been internalized by endocytosis, but they also receive biosynthetic cargoes from the TGN (i.e. precursors of lysosomal enzymes). Transmembrane proteins are sorted into topologically distinct limiting and intraluminal membranes, depending on their final destination (Fig. 6). ILVs accumulate downregulated receptors like EGFR, leading to the idea that inward membrane invagination process mediates the rapid extintion of signaling through sequestering the receptor from downstream cytosolic effectors [60].

Electron microscopic evidence suggests that the intralumenal vesicles of MVEs are formed through invagination and pinching-off of the limiting endosomal membrane [61]. Since vesicle budding process occurs in the opposite orientation compared with other budding events of cellular membranes (i.e. outwards from the cytosol), the molecular machinery involved must be different. ILVs biogenesis, as well as the sorting of ubiquitinylated cargo seems to be regulated by PI3P, in part through the adaptor protein HRS (hepatocyte growth factor regulated tyrosine kinase substrate). HRS is recruited to PI3P containing membranes via a FYVE domain, and it also contains an ubiquitin-interacting motif that binds ubiquitynilated cargo [62]. Down-regulation of HRS in mammalian was shown to lead to a decrease in the number of ILVs observed in endosomes [63].

Ubiquitinylated cargo interacts sequentially with ESCRT-I, -II and –III and eventually appears within ILVs present in MVBs [64]. ESCRT-I seems to be involved in the membrane deformation process. Knock-down of the ESCRT-I subunit Tsg101 (tumor susceptibility gene 101) causes pleiotropic changes in early endosomal morphology including reduction in the number of ILVs [58]. Moreover, both Tsg101 and Alix, a cytosolic adaptor protein, have been shown to regulate the budding of ILVs *in vitro* [65].

Accumulating evidence indicates that ESCRT-III complex and the ATPase Vps4, represent a highly conserved system for this type of membrane fission [66]. Two ESCRT-III subunits can assemble into helical tubular structures, while Vps4 binds inside the tubules, which are disassembled upon ATP

hydrolysis. Such helical structures presumably assemble within the neck of a forming ILV, catalyzing ILVs budding under Vps4 control.

Late endosomes

Late endosomes, which are more acidic then early endosomes (pH ~5.0-5.5), are also pleiomorphic, consisting of tubular, cisternal and vesicular elements with numerous membrane invaginations. They function as the second major sorting station in the endocytic pathway, wherefrom proteins and lipids can be returned to TGN, recycled to the plasma membrane or delivered to lysosomes for degradation.

Late endosomal limiting membrane, similar to the lysosomal membrane, contains high amounts of lysosomal associated membrane protein 1- and -2 (LAMP1 and LAMP2), which are believed to be protected from the degradative environment of the compartment because of their highly glycosylated state. LEs also contain $PI(3,5)P_2$, synthesized from PI3P by the PI3P 5-kinase PIKfyve, which has a crucial role in protein trafficking along the endocytic pathway. PIKfyve effectors have been recently identified, and include proteins involved in the control of protein sorting to lysosomes, such as components of ESCRT-III complex. Internal membranes of LEs in higher eukaryotic cells accumulate large amounts of LBPA, which is not detected on the outer face of the limiting membrane. LBPA is a highly hydrophobic, acid phospholipid that accounts for about 15% of the total late endosomal phospholipids, it is an inverted cone-shaped lipid, a structure that may facilitate the formation of the invaginations in LEs [67].

Interestingly, some late endosomal ILVs have the capacity to fuse back with the limiting membrane of the compartment by a mechanism called back-fusion. Through this process, proteins and lipids present within ILVs can be returned to the limiting membrane for further export to other cellular destinations. This is, for example, the case of mannose-6-phosphate receptors (M6PR) transiting through late endosomes during their cycle with TGN (Fig. 6) [68].

Fusion events within ILVs seem to be regulated both by cytosolic and luminal components, such as LBPA and its cytoplasmic effector ALIX. Interfering with LBPA functions leads to the sequestration of M6P receptors within these vesicles and inhibits cholesterol export from endosomes, mimicking the cholesterol storage disorder Niemann-Pick type C disease [69]. However, ALIX and LBPA may be mechanistically coupled to ESCRT functions, since ILVs formation in LEs and vesicles back-fusion depends also on the ESCRT-I subunit Tsg101 [65, 70]

Recent data suggest that late endosomes contain two different ILVs subpopulations, one enriched in LBPA which is endowed with the capacity of back-fusion, while the other is targeted for lysosomal degradation [71, 72]. Consistently, LBPA is strikingly resistant to lipases and phospholipases, perhaps because of its uncommon stereo configuration.

Lysosomes

Lysosomes, are the primary catabolic compartments of eukaryotic cells that degrade extracellular material internalized by endocytosis and intracellular components sequestered by autophagy. Lysosomes are membrane-bound organelles with an acidic (pH 4.6-5.0) luminal environment, due to the presence of proton-pumping vacuolar ATPases, and represent the terminal degradative compartment of endocytic pathway. The boundary between late endosomes and lysosomes is very elusive, lysosomes can only be identified by their physical properties on gradients and their electron-dense appearance and by the fact that they lack proteins found in LEs, including M6PR in transit, the small GTPase Rab7 or phosphorylated hydrolase precursors. It is well established that endocytosed macromolecules are delivered to lysosomes after their sequential passage through late compartments. However, the mechanism of endocytic cargo transfer remains controversial, and some mechanisms have been proposed. The maturation model proposes that LEs gradually enrich in lysosomal and loose late endosomal components, even though it is still not clear how lysosomes undergo content mixing with late endosomes. The vesicular model suggests that vesicles may bud from the late endosomes delivering their content to the lysosomes. Recently the kiss-and-run model has been proposed, and is supported by live-cell microscopy data showing that a continuous cycle of transient contacts followed by dissociations between endosomes and lysosomes contribute to cargo delivery [73]. Finally, the hybrid model suggests that endosomes and lysosomes may permanently fuse to for a hybrid organelle that contains both lysosomal and late endosomal components. Lysosomes are then reformed by the selective retrieval for LEs components. [74].

Lysosomal lumen is enriched in acid hydrolases involved in the degradation of proteins and lipids. In mammalian cells, newly synthesized lysosomal acid hydrolases were shown to be delivered to degradative compartments from the TGN.

Anthrax toxin trafficking along the endocytic pathway

Endocytic pathway is indeed a complex and highly regulated network. Extensive research over the last decade has shown that toxins evolved to hijack most, if not all, endocytic pathways to enter cells, including clathrin-dependent endocytosis, caveolae, and non-clathrin non-caveolar routes. Some of these pathways were actually uncovered through studies on bacterial toxins [6]. Therefore, it remains to be discussed what is known about which specific compartments of the endocytic pathway are involved in anthrax toxin entry and which membranes are involved in toxin translocation.

Upon toxin binding, the toxin-receptor complex is redistributed at the cell surface to specialized domains rich in cholesterol so-called lipid rafts. Association with lipid rafts was shown to be indispensable for efficient endocytosis [75]. It was recently shown that PA binding and its subsequent heptamerization triggers intracellular signaling events to allow recruitment of the endocytic machinery. Upon PA binding, activation of cellular src-like kinases (SLKs) takes place, which in turn cause the phosphorylation of the

cytoplasmic tail anthrax receptors. This event allows receptor ubiquitination by the The E3 ubiquitin ligase Cbl on a juxtamembranous lysine (K352 in TEM8 and K350 in CMG2) [30]. These modifications are necessary for the internalization of the toxin-receptor complex and rapid uptake. Accordingly, although endocytosis of the toxin-bound receptor is rapid, that of the toxin-free receptor is slow [76], indicating that toxin-receptor endocytosis is ligand triggered. Upon ubiquitination, the toxin-receptor complex is supposedly packaged into clathrin-coated vesicles as suggested by the dependency of the endocytosis process on the small GTPase dynamin and on the clathrin accessory protein Eps15 [75]. However, a direct role for clathrin has not yet been shown**.** Moreover, other cellular endocytic pathways have also been implicated in toxin uptake [77, 78].

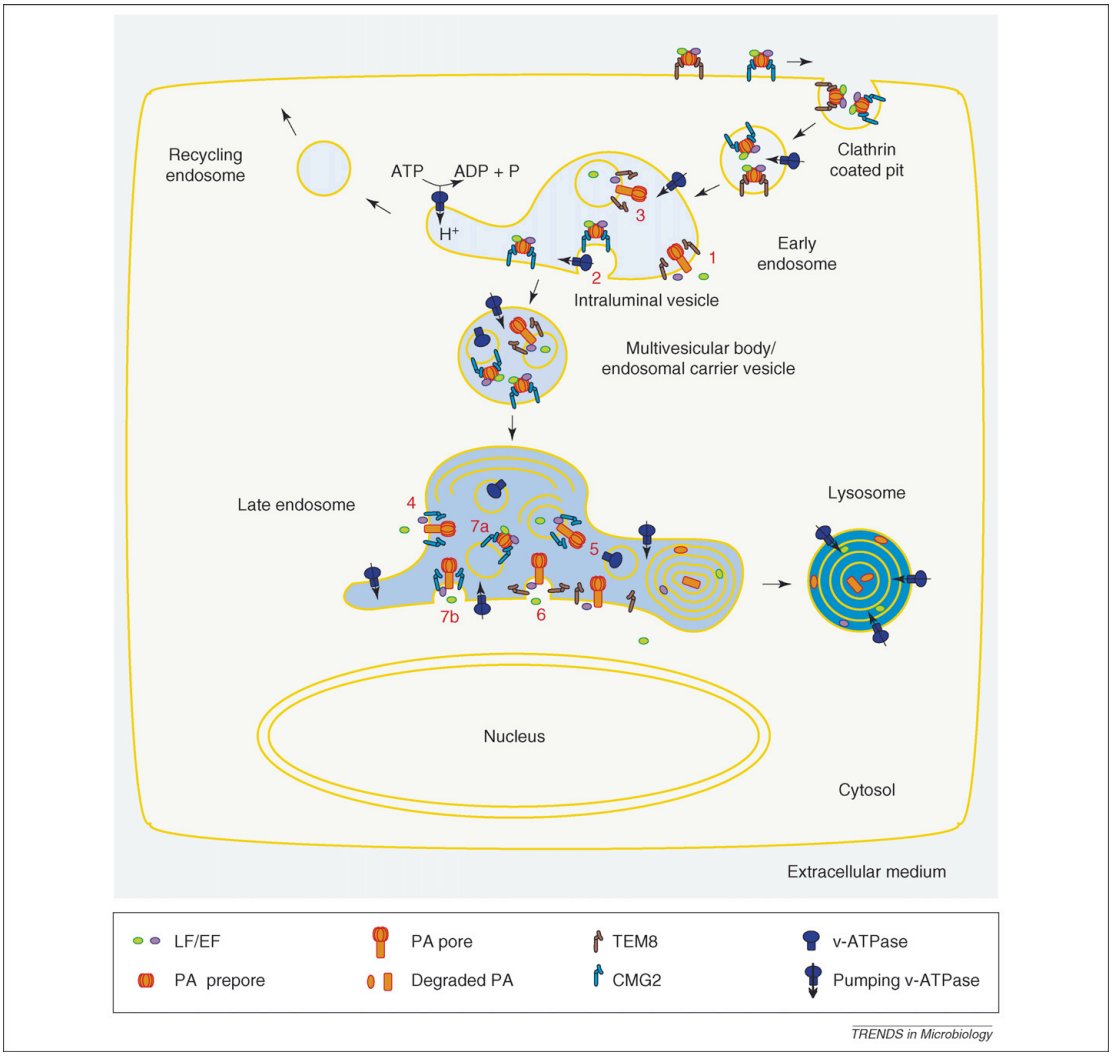

Fig. 7 *Anthrax toxins intracellular trafficking.* The possible routes for anthrax toxins along the endocytic pathway are summarized in this picture. Upon toxin-receptor complexes endocytosis, PA can insert in the early endosomal limiting membrane (1) or ILVs membrane (3), the latter resulting in the delivery EF/LF in the lumen of ILVs. Sorted to LEs, EF/LF can be delivered to the cytosol by ILVs backfusion (6) or by PA mediated translocation across the limiting membrane (4) [5].

Although anthrax toxin cell entry fits the general scheme of cytosolic delivery of bacterial toxins exploiting the endocytic route, it reveals unique features. Most models of cell entry of endocytosed bacterial toxins depict the toxin-receptor complex on the luminal side of the endosomal limiting membrane, wherefrom the toxin translocates into the cytosol upon acidification, as was established for diphteria toxin (DT). Conversely, this does not seem to be the case for anthrax toxin.

An additional, perhaps predominant form of cytosolic delivery was suggested for anthrax toxin (Fig. 7). It was found that once anthrax toxin is taken up by the cell and delivered to early endosomes, it is preferentially incorporated into intraluminal vesicles formed by invagination of the endosome limiting membrane [79]. When the pH-triggered membrane insertion of $(PA_{63})_7$ occurs on ILVs membranes, translocation of EF and LF leads to their release into the lumen of ILVs, still away from their cellular targets. At the late endosomal stage a population of ILVs can undergo back-fusion with the limiting membrane [71] leading to the release of EF and LF into the cytoplasm. It is noteworthy that being segregate to ILVs, which are thought to be topologically equivalent to cytosol, EF and LF would be sheltered from acidic proteases and hydrolases that reside in the lumen of LEs.

Although the involvement of ESCRT proteins has not been addressed for anthrax toixn, this model is supported by biochemical data in different cell types. In particular, subcellular fractionation studies showed that the SDS-resistant PA_{63} heptamer, which only forms after the pH-dependent conformational change, is highly enriched in early endosomes, indicating that insertion into the membrane already occurred in early compartments [79]. Interestingly, in the same study, it was reported that late endosomes are involved in LF entry into the cytosol because MKK1 cleavage was negatively affected by inhibitors of membrane trafficking from EEs to LEs and cell fractionation of BHK-21 cells detected intact LF in LEs. Similarly, EF was found in LEs [80]. Moreover, LF-catalyzed MKK1 cleavage was observed only after 30 minutes in RAW264.7 cells [81]. Likewise, the increase of cytosolic cAMP levels induced by EF was measured with different techniques in different cell types and in all cases, cAMP began to rise only 30-40 minutes after toxin addition [80], a time course consistent with the involvement of LEs in EF and LF delivery to the cell cytosol. Finally, it has been shown that interfering with the development and dynamics of ILVs (and thus of MVBs and LEs) delays LF mediated cleavage of MKKs. This mechanism was recently proposed for vesicular stomatitis virus (VSV) entry into target cells [82].

However, MKK1 cleavage has been also reported to occur within 10-15 min after endocytosis of PA and LF in Chinese hamster ovary (CHO) cells, a time course consistent with LF exiting from EEs [79]. Much debate is emerging on the site from where EF and LF exit the endosomes since available data are contradictory. Up to now, it seems that the two enzymatic subunits of anthrax toxin exit from endosomal compartments at various stages of the endocytic route, more likely and predominantly from LEs by ILVs back-fusion, but the relative contributions of EEs, MVBs and LEs as subcellular sites of entry into the cytosol remain to be fully established.

EF and LF cytoplasmic localization

It has been reported that EF, after translocation into the cytosol, generates a cAMP concentration gradient from the perinuclear area to the cell periphery [80]. The gradient was observed to be sustained in time rather than transient, suggesting it may be the consequence of EF being associated to the cytosolic face of late endosomal membranes it translocated from. Conversely, after translocation LF is believed to diffuse away into the cytosol and where it cleaves MKK isoforms that reside in different cellular compartments [81]. Accordingly, upon subcellular fractionation, EF was found within the late endosomal fraction, whereas LF was found in the cytosolic fraction [80]. Moreover, EF was shown to strongly interact with liposomes *in vitro* at neutral pH, which is not the case for LF and PA_{63} [83]. However, further experiments need to be done in order to confirm the model suggesting different localization for EF and LF after cytosolic delivery.

2.4 Anthrax toxin cellular and systemic effects

Once in the cytosol, EF and LF have access to their respective intracellular substrates and cofactors. EF can bind calmodulin, converting ATP to cAMP, and LF can cleave MAPKKs, resulting in the alteration of two major cellular signaling pathways, thereby promoting anthrax pathogenesis.

The precise role of the two toxins in anthrax pathology remains to be fully elucidated. Earlier studies suggested that the toxins were responsible for death [13, 84] but recent studies indicate they play a key role in early stage of infection, in fact their primary targets seem to be cells of innate and adaptive immunity that would otherwise impair the multiplication of the bacilli [14, 15]. The two toxins would then act on many different cell types, when they accumulate to high levels in the circulation during the final stages of the disease, following the dissemination of *B. anthracis* in the infected animal, where they might elicit toxic systemic effects. Accordingly, it is interesting to note that anthrax toxins target ubiquitous receptors, expressed by different cell types and tissues [31].

Lethal factor: cellular effects

LF is a highly specific protease that cleaves mitogen-activated protein kinase kinases (MKKs). MKKs are cytosolic proteins that lie in the middle of phosphorylation cascades activated by a wide variety of cellular stimuli including growth factors, cytokines and stress [85]. MAPK cascades are typically organized in a three-kinase architecture consisting of the upstream mitogen-activated protein kinase kinase kinases (MKKKs), which activate mitogen-activated protein kinase kinases (MKKs), which in turn activate mitogen-activated protein kinases (MAPKs). Transmission of signals is achieved by sequential phosphorylation and activation of the components specific to a respective cascade. MAPKs

phosphorylate a large number of cellular targets and play a crucial role in mediating responses to extracellular signals, including changes in the transcriptional profile.

In mammalian systems, five distinguishable MAPK modules have been identified so far. These include the extracellular signal-regulated kinase 1 and 2 (ERK1/2) cascade, which preferentially regulates cell growth and differentiation, as well as the c-Jun N-terminal kinase (JNK) and the p38 MAPK cascades, which function mainly in stress responses like inflammation and apoptosis [86]. In eukaryotic cells, MKK isoforms are seven (MKK1-7) and integrate signals from at least 20 MKKKs and are exclusive to particular MAPK families. LF proteolytic action is targeted to all mammalian MKKs except for MKK5, thereby its action shuts down the ERK, JNK and p38 pathways in infected cells.

LF cleaves MKKs at specific sites outside of the catalytic domain, disrupting or removing a MAPK-docking motif also called D-site on MKKs N-terminal. MKKs lacking the D-site are unable to bind their cognate MAPK with high affinity, and thus LF cleavage inhibits MAPK phosphorylation by MKKs upon stimulation. LF recognizes MKKs via multiple interactions, which include the cleaved N-terminal tails and other regions. Recently, an LF interacting region essential for LF-mediated cleavage was identified within the C-terminal kinase domain of MKK1 [87, 88]. The alignment of the N-termini of the cleaved MKK isoforms defines a consensus motif for the cleavage site consisting of one to four positively charged and two hydrophobic residues. A surface complementary to MKKs N-terminus exists in LF active site within a deep groove with an overall negative charge, placing the peptide bond to be cleaved into the continuous active site center [21]. The encounter of LF with its targets might be slightly problematic due to a low intracellular abundance of MKKs. However, although MEK can be found in the cytoplasm, increasing evidence indicates that scaffolding complexes lead to specific association of signaling molecules with a given organelle, in particular those of the endocytic pathway [89].

Edema factor: cellular effects

EF is an extraordinarily active calcium- and calmodulin (CaM)- dependent adenylate cyclase (AC) which raises intracellular cAMP levels.

Signaling through cAMP governs many fundamental cellular functions, including metabolic, electrical, cytoskeletal, and transcriptional responses within the cell. In all eukaryotic cells, cAMP is generated from ATP by two families of class III AC. One family comprises of transmembrane ACs, which play key roles in cellular responses to extracellular signals. They are modulated through heterotrimeric G proteins in response to stimulation of G-protein coupled receptors (GPCRs). The second family encompasses cytoplasmic enzymes referred to as soluble ACs, which are directly activated by calcium and the cellular metabolites bicarbonate and ATP. The biological effects of intracellular cAMP increase are mediated by cAMP binding to three families of signal transducers: cAMP-dependent protein kinases, cyclic nucleotide-gated channels and exchange protein directly activated by cAMP (EPAC). cAMP is

eventually broken down to 5'-AMP by cyclic nucleotide phophodiesterases (PDEs). The delicate balance between cAMP formation by ACs and degradation by PDEs determines cellular cAMP levels.

Many pathogenic bacteria produce toxins that perturb this balance by raising intracellular cAMP levels in host cells, mainly through two major mechanisms. The first mechanism is by the action of the bacterial adelylyl cyclase (AC) toxins, which possess AC activity. AC toxins are activated only upon their entrance into host cells and association with the specific cellular proteins that serve as activators. In addition to EF from *Bacillus anthracis*, two other examples of AC toxins are CyaA from *Bordetella pertussis* and ExoY from *Pesudomonas aeruginosa*. The second mechanism used by bacteria to increase intracellular cAMP is the ADP-ribosylation of heterotrimeric G proteins by bacterial toxins, resulting in increased catalytic activity of host membrane-bound AC. Cholera toxin from *Vibrio cholerae* can ADP-ribosylate $G_S\alpha$ subunit of heterotrimeric G protein, making it constitutively active to stimulate host membrane-bound AC. *Bordetella pertussis* pertussis toxin targets a different G protein subunit, $G_i\alpha$, uncoupling G protein-coupled receptor from inhibiting host membrane-bound ACs thus resulting in increased cAMP levels.

Once delivered to the cytosol of host cells, EF binding to calmodulin must be facilitated by the high abundance of calmodulin (1% of total cellular proteins). EF binding to CaM is irreversible and very different from that of the non-pathological CaM-interacting proteins.

EF was shown to have at least 1,000 fold higher AC activity than those of class III AC, which comprises mammalian ACs [23, 90]. Structural and simulation studies reveal that both classes of AC share the same reaction mechanism [4]. However, it was shown that the motion required for the activation of EF and CyaA is significantly smaller than that of mAC [22]. Moreover, there are fundamental differences at the catalytic site, which would dictate their ability to lower the transition state energy [23].

By increasing cAMP levels, EF inhibits also MAPK-dependent gene expression, highlighting a crosstalk between the cellular action of EF and LF. Following cAMP binding, PKA inhibits the Raf-MKK-Erk pathway by phosphorylating a negative regulatory residue of Raf. In addition, PKA blocks the MKK4-JNK and MKK7-JNK pathways by inhibiting the initial small GTPase Rho. Finally, PKA inhibits signaling through receptors coupled to Src family protein tyrosine kinases by activating the specific inhibitory kinase Csk. PKA can also modulate gene expression by tranlsocating into the nucleus and phosphorylating cAMP-responsive transcription factors, such as CREB.

Anthrax toxin action on the immune system

All bacterial pathogens have to deal with the host immune system. Regardless of the route of entry, *Bacillus anthracis* needs to keep the immune system at bay to achieve effective colonization, but at the same time it needs to rely on host's phagocytic cells, used to reach the lymph node wherefrom the

bacteria eventually enter the lymphatic and blood circulation, rapidly causing massive bacteremia and toxemia [15]. Hence the activity of phagocytic cells must be not only intact, but possibly enhanced at the onset of infection. On the other hand, both the innate and the adaptive immune defenses must be suppressed when bacteria reach lymph nodes. This transition seems to be marked by expression of the anthrax toxins, which paralyze immune system to establish a protected environment where bacteria can multiply. This state of immunosuppression is not permanent, as shown by the development of a potent humoral response against the receptor-binding component of the toxins in the anthrax survivors of the bioterrorist attacks in 2001 [91].

LeTx was shown to inhibit the production of several pro-inflammatory cytokines and nitric oxide in macrophages, both *in vitro* and *in vivo*, neutralizing macrophage activation induced by bacterial components of *B. anthracis*. Moreover, while EdTx enhances spontaneous macrophage migration [92], both LeTx and EdTx inhibit macrophage chemotaxis through the respective enzymatic activities. [93]. This function is likely to result in suppression of the migratory response of macrophages towards inflammatory chemokines produced at the site of infection. Furthermore, LeTx induces rapid cytolysis of murine macrophages from some imbred mice. Different mouse strains display markedly different susceptibility to LeTx dependent cytolysis, suggesting that this process might be independent of MKKs cleavage [94] and leading to the identification LeTx sensitivity locus as Nalp1b. This gene encodes a polymorphic inflammasome component that has been highlighted as a potential target of LF [95]. Surprisingly, CREB is a crucial target for the maintenance of macrophage survival in the context of the LeTx induced LTR4-dependant cell death. EdTx has been shown to rescue macrophage cells from apoptosis via the downstream activation of protein kinase A (PKA) and CREB [96].

Similarly to macrophages, LeTx induces the apoptosis of murine DCs *in vitro* and *in vivo* [97]. Interestingly, DCs become resistant to LeTx killing during maturation. Hence, immature DCs in peripheral tissues can be killed by LeTx, while mature DCs in the lymph nodes are unaffected. LeTx has inhibitory effects on DCs pro-inflammatory cytokine secretion (TNF-α and IL-6) [98]. Interestingly, EdTx and LeTx were found to cooperate in inhibiting TNF-α production, while the expression of IL-12p70 (Th1 poliarizing) and IL-10 (th2 activation inhibiting) is suppressed differentially by EdTx and LeTx. [99]. Anthrax toxin may finely tune the balance between signals delivered by DCs, inducing terminal differentiation of T cells towards a Th2 rather than Th1 immune response.

Although impairment of DC activation and maturation would be by itself sufficient to prevent the development of the response against the pathogen mediated by T and B lymphocytes, *B. anthracis* also affects the activation and effectors functions of these cells through the combined activity of EdTx and LeTx. In fact, PA was shown to bind to both T and B lymphocytes, identifying these cells as targets for EdTx and LeTx [15]. T cell activation is suppressed directly by LeTx and indirectly by EdTx. Through the production of cAMP, EdTx perturbs PKA-dependent signaling pathways including MAPK cascade,

which represents therefore a common target on the anthrax toxins. Both EdTx and LeTx have been reported to suppress T cell chemotaxis through suppression of Erk1/2 activation. [93].

Although the activation of antigen-specific B cells requires T-cell help, *B. anthracis* can also inhibit B cells activation directly by targeting the MAPK pathway. In fact, LeTx inhibits B cell proliferation and antibody production *in vitro* and *in vivo* through MAPK cascades inhibition. This effect has been reported to correlate with the cleavage of MKK1, MKK2, MKK3 and MKK4 [100].

Anthrax toxin action on epithelial and endothelial cells

After the first stages of infection, when they seem to act mainly on the host immune system cells, EdTx and LeTx act on many different cell types. Owing to the ubiquitous nature of receptors, most cells are able to internalize the toxin and to be damaged by MKKs cleavage and elevated cAMP levels.

Although the effects of LeTx on endothelial cells have not been directly investigated *in vivo*, many studies indicate that LeTx affects angiogenesis and tumor vasculature, supporting a targeting of the endothelium of the host [101, 102]. LeTx was shown to induce endothelial cell-death independent permeability in zebrafish vasculature with associated pericardial edema and this effect was linked to MKK1-2 cleavage by the toxin [103]. Moreover, it was shown that LeTx can induce a cell-death independent loss of barrier function *in vitro* on endothelial cells [104]. The role of MKKs cleavage in endothelial cell dysfunction need to be further investigated. These types of effects are likely not relevant to LeTx-mediated lethality and vascular collapse, which are cytokine-dependent, but play an important role in bacterial infections which are accompanied by strong cytokine production.

A recent study on LeTx effects in human lung epithelial cells reports LeTx mediated decreases in transepithelial electrical resistance and loss of barrier function. This has been shown to be associated with the alteration of cellular tight junctions and focal adhesions over days of toxin treatment [105]. LeTx effects observed are due to increases in F-actin levels in cells and these cytoskeletal changes seem to be induced by MKKs cleavage by LeTx. However, the toxin-mediated remodeling of the lung epithelium still needs to be verified *in vivo*. Nevertheless, it is unlikely these effects contribute to LT-mediated lethality, but they may suggest similar cytoskeletal-mediated changes linked to barrier function alterations in endothelial cells [101].

EdTx and LeTx combinatorial effects

Because their expression is coordinately regulated, EdTx and LeTx circulate together during infection. The two toxins target a similar spectrum of cell types but they have different catalytic activities, suggesting they may impair cell functions in a synergistic manner. EdTx and LeTx have been shown to cooperate in inhibiting superoxide production by neutrophils, cytokine secretion by DCs, antigen-receptor dependent T cell activation and proliferation.

However, EdTx appears to counteract macrophage apoptosis induced by LeTx. EdTx activates CREB, which is a macrophage survival factor downstream p38. LeTx in turn inhibits the p38 pathway through MKK3/6 cleavage and many of LeTx effects in cells are due to the impairment of this pathway. EdTx activation of CREB has been shown to promote survival of LeTx treated macrophages that normally would undergo apoptosis [96].

It should be pointed out that it is very difficult to design experiments to study combinatorial effects of EdTx and LeTx because it is challenging to model the complex events that occur *in vivo* during infection. The relative amounts of each toxin, timing and site of production, and factors affecting toxin binding and uptake are still unknown for most stages of anthrax infection. EdTx and LeTx display immunosuppressive effects *in vitro* at concentrations in the range that can be measured in the blood during systemic phase of anthrax infection [106]. However, there are still no information about the concentration of EdTx and LeTx that accumulate locally.

Furthermore, it has been recently shown that EdTx causes up-regulation of the PA receptors TEM8 and CMG2, specifically in macrophages, thus increasing the sensitivity to anthrax toxin cytotoxicity [32, 33].

In vivo studies

Despite the recent advances on the understanding of LeTx and EdTx effects on many cell types *in vitro*, the involvement of MAPK and cAMP signaling pathways in multiple cellular functions in virtually every cell type of the host makes it very difficult to identify the crucial and relevant *in vivo* targets for LeTx and EdTx during infection.

Before the major advances in molecular and cellular biology, anthrax toxin research began in the 1960s with the observations made by Smith and colleagues on toxin-mediated effects on animals infected with crude toxin preparations. Intravenous delivery of LeTx was shown to kill rodents and other mammals (from here, the name lethal toxin), albeit with significant differences in potency among different strains and species. In contrast, EdTx was non-lethal, but produced edema upon subcutaneous administration (from here, the name edema toxin).

The availability of highly purified recombinant toxin preparation has allowed this earlier works to be revisited in a more systematic manner. Death from LeTx treatment in mice is associated with shock, vascular collapse and generalized hypoxia, reminding of some of the symptoms seen in human inhalational anthrax patients. LeTx induces an atypical vascular collapse in mice and rats without classic hallmarks of endotoxic shock, marked by absence of thrombosis or cytokine involvement but it is still not known how it is induced. In contrast, EdTx used at doses that are lethal for mice is associated with hemorrhaging lesions in many organs accompanied by hypotension and bradycardia [101]. It is noteworthy that LeTx-induced vascular shock kills mice with LeTx resistant macrophages as well as macrophage-deficient mice.

An important issue to address is the dose relevance of toxins secreted by the bacterium in infected animals. Recently, a detailed analysis of *in vivo* toxin production levels in anthrax infected rabbits pointed out a 5:1 ratio of LF:EF in most samples [106]. This finding confirms what was reported for *in vitro* toxin prodution (PA:LF:EF 20:5:1) [107]. Based on the 5:1 ratio, it is likely that lethal doses of EdTx in mice are actually not achieved in infection. Indeed, further studies on the timing and levels of toxins produced by *B. anthracis* in early stages of infection will address this issue.

Aims of the project

Two toxins released by *Bacillus anthracis* are the major virulence factors involved in the pathogenesis of anthrax. They are large multi-domain proteins that include an enzyme that alter two major signalling pathways in a variety of cells, included the cells of the immune response. They are the lethal factor (LF) which proteolytically cleaves the MAPK kinases and the edema factor (EF) an adenyate cyclase which greatly elevates the level of cAMP inside the cells. They bind to the cell surface via the protective antigen (PA) and enter the cytosol via the endosomal route. Anthrax toxins play a key role during *Bacillus anthracis* mediated infection and therefore the understanding of how anthrax toxins enter the cell and display their activity in the cytosol is of paramount importance. For two reasons: to acquire a better knowledge of this key event in infection and to devise novel inhibitors and protocols to prevent the development of the disease. Moreover, studying the mechanisms of action of microbial virulence factors not only reveals their mode of operation, but also highlights important features of the affected host target, because virulence factors have been shaped, by evolution, around that particular target molecule and function. Addressing anthrax toxin trafficking through the endocytic pathway may also clarify important aspects involved in mammalian cells vesicular trafficking, such as the molecular machinery and regulation involved in late endosomes function and localization. More in details, this project aimed at testing the possibility that the two anthrax toxins enter inside intralumenal vesicles of the early endosomes, wherefrom they enter the cytosol via back-fusion taking place at the level of late endosomes.

To date, the process of entry of EF and LF has been studied using indirect methods such as cholesterol depletion, cross linking, siRNA, over-expression of proteins involved in endocytosis and vesicular dynamics, which may however alter the physiological process of cell entry of this toxins.

At variance, the present project envisaged to generate fluorescent chimera of LF and EF with fluorescent proteins of different colors and to video-image chimeric fluorescent EF and LF to visualize and localize the two anthrax toxins within the live cell, whose physiology is not altered in any way.

A particular focus of this project was that of localizing the activity of EF and LF after cytoplasmic delivery. EF seems to associate to the cytosolic face of late endosomal membranes while LF appears to diffuse into the cytosol, judging from the range of MAPK kinase isoforms which are cleaved by this toxin. Taking into account the relevance of compartmentalization of cellular signaling, addressing this issue will point out a role also for compartmentalization of toxin activity.

Up to now, this evidence is based on observations on the localization of EF activity in cultured cells with a FRET based cAMP sensor. LF localization was deduced by cellular fractionation, and one cannot exclude the possibility of a toxin redistribution among fractions after cell fragmentation. One purpose of the present project was that of imaging cytosolic localization of chimeric EF and LF fused to fluorescent proteins after their cytoplasmic delivery. Moreover, in order to compare LF activity dynamics with those of EF, we were interested in developing a tool for studying LF intracellular spatiotemporal activity in single cell, as it was done for EF using a FRET based cAMP biosensor [80].

A third point was that related to the fact that no data were available on the nature of EF binding to the cytosolic face of the endosomal membranes and on the toxin domain involved in such interaction. To address these questions we planned to study the interaction of EF and LF with isolated endosomal membranes *in vitro* by Surface Plasmon Resonance (SPR), which has recently emerged as one of the most important techniques for studying macromolecular interactions. Moreover, SPR has been used to study membrane-protein interactions and it has given information on important processes such as the binding of domains or proteins that participate in cell signaling or the initial membrane attachment of pore-forming protein. In order to establish which EF domain is involved in the protein localization on endosomal membranes, we planned to use a domain swapping approach. EF and LF with swapped N-terminal domains and fused to fluorescent proteins were designed and imaged in cultured cells by fluorescence microscopy.

Results and discussion

1. Anthrax toxin intracellular trafficking along the endocytic pathway

EF and LF fluorescent chimeras

Four chimeras EF-EGFP, EF-mCherry, LF-EGFP, LF-mCherry were previously produced as recombinant molecules, consisting of the full length EF and LF fused at their C-termini to different fluorescent proteins: enhanced green fluorescent protein (EGFP) or monomeric Cherry (mCherry) fluorescent protein [108]. Fusion at the N-terminus was avoided because, in both EF and LF, this domain is essential for PA-binding and translocation across the channel. The recombinant proteins were produced with an N-terminal 6xHis tag, which allows easier purification by affinity chromatography and was shown to confer to LF an increased capacity to enter and translocate across the $(PA_{63})_7$ transmembrane channel [49]. In particular, the N-terminal of bound LF or EF enters the $(PA_{63})_7$ pore under the influence of acidic endosomal pH and positive membrane potential. By protonating His residues, low pH is predicted to destabilize LF N-terminus, giving the N-terminal flexible region of LF and EF a net positive charge, which has a role in initiating the threading of ligands into the $(PA_{63})_7$ pore.

Fig. 1 *Fluorescent chimeras schematic representation*

EF and LF fluorescent chimeras activity in cultured cells

In order to perform fluorescence microscopy experiments on cultured cells, the functionality of the two EF and the two LF derivatives WAS tested in the fibroblast baby hamster kidney (BHK-21) cell line. Even though fibroblasts are not the main target of anthrax toxins during infection, multiples are the reasons for the choice of BHK-21 cells as a model in this study. The main one is that endosomal membrane composition has been well characterized in this cell line [67]. Moreover, BHK-21 cells express both PA receptors, as the majority of sensitive cells do. Finally, their flattened shape favors single cell fluorescence microscopy analysis.

Enzymatic activity and kinetics in the cytosol of cultured cells were tested to ensure the quite big fusion proteins (~120 kDa) retained the ability to interact with $(PA_{63})_7$ prepore bound to the cell surface, to partially unfold to translocate across the narrow $(PA_{63})_7$ channel formed on endosomal membranes, and to maintain the capability to bind cellular substrates and exert EF and LF catalytic activity.

EF is an extraordinary active adenylate cyclase that raises intracellular cAMP levels. An efficient cAMP biosensor based on fluorescent resonance energy transfer (FRET) was recently designed [80]. In this study, the FRET probe was chosen to characterize EF derivatives activity in BHK-21 cells.

The FRET probe for cAMP was generated fusing the regulatory subunit (R) and the catalytic subunit (C) of the cAMP-binding protein kinase A (PKA) to the cyan (CFP) and the yellow (YFP) variants of the green fluorescent protein, respectively. In quiescent cells the R-CFP and C-YFP subunits are associated in a holotetrameric complex and FRET occurs among them, but cAMP induces their separation with loss of FRET signal.

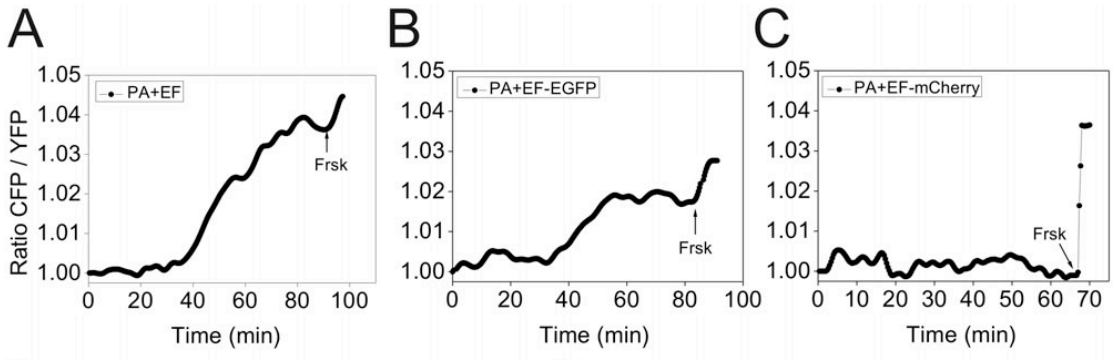

Fig. 2 *EFmCherry activity in cultured cells.* cAMP fluorescence resonance energy transfer imaging in transfected cells expressing the catalytic PKA subunit-YFP and the regulatory PKA subunit-CFP in the cytosol. BHK cells were imaged after treatment (time zero) with PA in combination with EF (A) or EF-EGFP (B) and EF-mCherry (C). Arrows indicate addition of forskolin (Frsk) as control at the end of experiments.

Fig. 2B shows that EF-EGFP retained its biochemical activity, rising cAMP levels 40 minutes after toxin addiction, with the same kinetics as the wild type EF. However, EF-EGFP seemed to reach lower levels

of activity respect to its unconjugated counterpart (Fig. 2A). On the contrary, EF-mCherry displayed no intracellular activity (Fig. 2C). Forskolin (Frsk), a potent activator of ACs, was added at the end of each experiment as a control.

LF is a highly specific protease that cleaves all MKK isoforms except for MKK5. Thus, to test if the fluorescent LF derivatives are functional in cultured cells, the time course of MKK3 cleavage in BHK-21 cells treated with PA and LF or LF-EGFP or LF-mCherry was observed. Total cell extracts were made at given time, and after SDS-PAGE the proteins were blotted and stained with anti MKK3 antibody (Fig. 3D), which detected two bands corresponding to two splicing isoforms of the protein. The one of lower electrophoretic mobility corresponds to isoform MKK3b (40 kDa). LF targets a unique site of cleavage (between residues 26-27) on the N-terminal region of MKK3b (Vitale et al., 2000). The second band at higher mobility corresponds to isoform MKK3a, which lacks the first 29 N-terminal residues, and thus is not susceptible to proteolysis mediated by LF. Upon cleavage, isoform MKK3b appeared downshifted and migrated in close proximity to isoform MKK3a. However, LF mediated proteolytic cleavage generates a MKK3b fragment easily distinguishable from its uncleaved form, thus permitting the accurate determination of the kinetics of proteolysis. The percentage of cleavage over time was quantified and normalized against the control (Fig. 3E). LF-EGFP was active in the cell cytosol, even though with slower kinetics with respect to the unconjugated LF, which started cleaving MKK3b 40 minutes after toxin addition. On the contrary, LF-mCherry was not active.

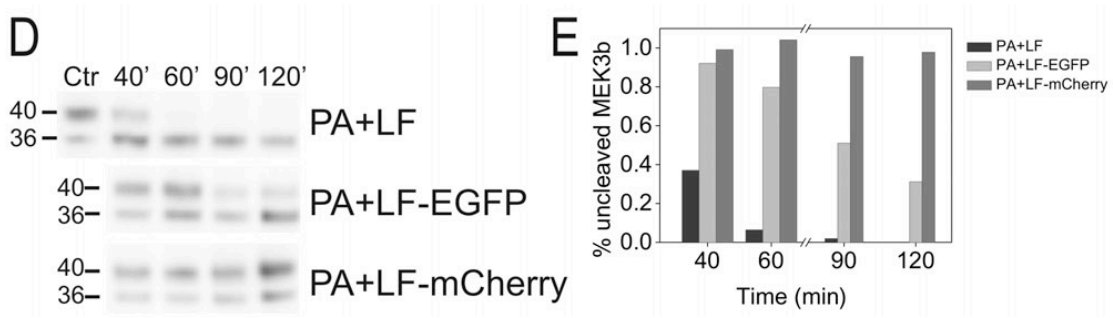

Fig. 3 *EF-EGFP activity in cultured cells.* Time course of MKK3b cleavage in BHK cells treated with PA and LF, or LF-EGFP or LF-mCherry. Total cell extracts were made at the given time, and after SDS-PAGE the proteins were blotted and stained with anti-MEK 3 antibodies (panel D). Panel E shows densitometric quantification of the bands expressed as ratio between the MEK3b band and the lower molecular weight band intensities, normalizing the result against the control.

Taken together, these data show that the EGFP derivatives of both LF and EF are active in the cell cytosol, implying they are able to interact with $(PA_{63})_7$ prepore on the cell surface, to translocate across the $(PA_{63})_7$ channel on endosomal membranes, and finally they reach the cytosol to exert their catalytic activity and therefore are able to report on each step of the cell entry process. However, both LF-EGFP and EF-EGFP showed lower levels of activity with respect to their unconjugated counterparts, probably

because a smaller number of molecules are capable of reaching the cytosol when EGFP is fused to the proteins. Interestingly, the two mCherry chimeras displayed no intracellular activity. The more likely explanation is that they are unable to unfold and translocate into the cytosol across the $(PA_{63})_7$ channel.

EF and LF fluorescent chimeras translocation across $(PA_{63})_7$ channel

Recombinant fluorescent chimeras bear the ~ 30Å large and ~ 40Å high rigid barrel of the EGFP or mCherry fluorescent proteins at their C-terminal, and they need pull the whole molecule across the narrow $(PA_{63})_7$ channel (~ 15 Å diameter). Fluorescent proteins (FPs) are ~26 kDa proteins that have a typical β-barrel structure, consisting of one β-sheet with α-helix(s) containing the cromophore running through the center. The tightly packed nature of the barrel makes FPs quite resistant to unfolding.

To test their ability to pass through $(PA_{63})_7$ channel, the translocation of EF and LF fluorescent chimeras across $(PA_{63})_7$ pores formed in planar phospholipid bilayers was measured. $(PA_{63})_7$ pores were inserted into the artificial membrane and EF, LF or their counterparts conjugated to fluorescent proteins were added. The progress of binding to $(PA_{63})_7$ channels was monitored by the decrease in conductance. Translocation was initiated by applying a pH and voltage gradient across the artificial membrane, mimicking the physiological conditions across endosomal membranes. The EGFP derivatives of both EF and LF translocated with slightly lower efficiency and time-course than the wild-type proteins, whereas the mCherry derivatives did not translocate at all (Fig. 4). These results are in agreement with the absence of cytosolic activity observed in BHK-21 cells treated with LF-mCherry and EF-mCherry (fig. 2 and 3). In this study it was not investigated in detail the reason for the difference between EGPF and mCherry behavior, but it is likely to be due to a different energy requirement for their unfolding. To test this hypothesis, *in vitro* unfolding of EGFP and mCherry exposed to increasing concentrations of the denaturing agent guanidine hydrochloride (GdnHCl) was measured.

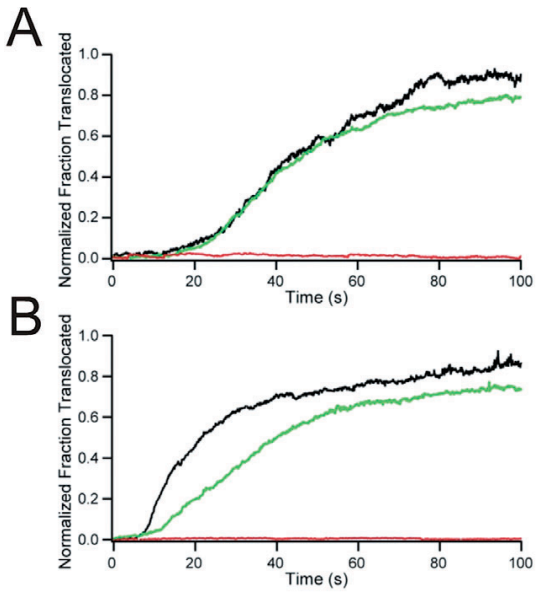

Fig. 4 *Translocation of chimeric proteins across artificial membranes*
Measurement of the chimeric proteins translocation across channels formed by PA63 in artificial planar phspholipid bilayer. (A) Translocation of LF (black) versus LF fused with either EGFP (green) or mCherry (red). (B)Translocation of EF (black) versus EF fused with either EGFP(green) or mCherry (red).

It is well documented and accepted that FPs fluorescence is intimately linked to their properly folded structure, as in the native structure the chromophore has restricted movement and is shielded from bulk water. Only when the FP is denatured, the chromophore has increased rotational freedom and also undergoes attack by water molecules leading to quenching of its fluorescence (Enkoi et al., 2004). Thus, unfolding curves for EGPF and mCherry were determined by exciting the samples at 365 nm and detecting the emitted fluorescence at appropriate wavelength. Fig. 5 shows that mCherry had a higher resistance to unfolding compared to EGFP when exposed to GdnHCl, confirming that despite having very similar structures, the two FPs have different structural stability, mCherry having the highest.

Protein unfolding has been documented to be necessary for the translocation across $(PA_{63})_7$ channel and this result provides a further example. Accordingly, only EF-EGFP and LF-EGFP were used in the study of the final stage of intoxication. Finally, this study shows that mCherry may not be an appropriate choice as a reporter of intracellularly acting toxins.

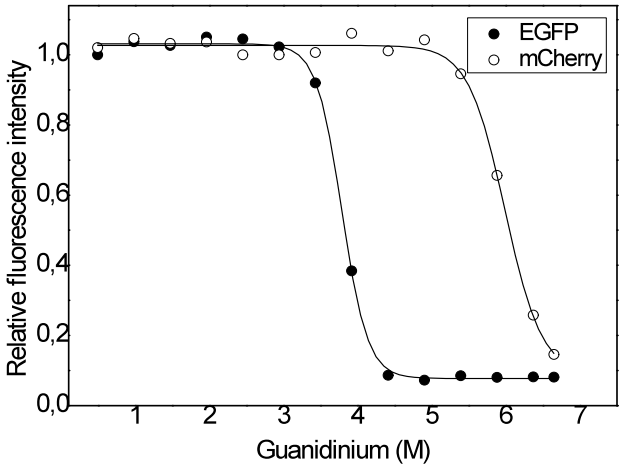

Fig. 5 *EGPF and mCherry unfolding curves*
Fluorescence intensity changes for EGFP and mCherry due to protein unfolding when exposed to increasing concentrations of guanidine hydrochloride (GdHCl). The samples are excited at 365 nm and the emitted fluorescence is detected at 510 nm and 610 nm, for EGFP and mCherry, respectively.

Endocytosis of EF-EGFP and LF-EGFP

In this study, the intracellular trafficking of fluorescent EF and LF chimeras in cultured cells has been analyzed by fluorescence microscopy. Particular attention was paid on using experimental conditions that simulate the *in vivo* situation, in order to avoid manipulations that could potentially distort the normal dynamics of anthrax toxin endocytosis. Many studies have been performed incubating target cells at low temperatures in order to inhibit endocytosis, and then shifting to 37°C to ensure a synchronized-like cell entry of the toxins. Conversely, in this study the chimeric toxins were added to cultured cells at 37°C in order to avoid the cell shape change that takes place when cells are shifted from a cold environment to 37°C. Moreover, the use of anthrax receptors TEM8 and CMG2 over-expressing cells was prevented in order to avoid the possibility that a high receptor density would alter the picture of toxin cell surface binding by creating clusters of PA receptors.

BHK-21 cells were treated with PA and EF-EGPF or LF-EGPF at 37°C. Cells were fixed at different time points (3, 5, 10, 40 minutes) after toxin addition, specific cellular markers were stained by immunofluorescence and the samples were observed by fluorescence microscopy. The strength of the fluorescent signal was not optimal, due probably to the low amount of toxin which actually enters the cell during intoxication, therefore it was amplified using anti-GFP antibodies, and it was assessed not to alter the pattern of fluorescent distribution.

Early endosomes

After 10 minutes of incubation (Fig. 6) both toxins were observed by fluorescence microscopy within early endosomal compartments that contain phosphatidylinositol 3-phosphate (PI3P) and Rab5, but apparently no transferrin (Tfn) or early endosomal antigen 1 (EEA1).

Controls with equimolar amounts of PA and EGPF were performed (not shown) and revealed no fluorescence staining, indicating that the observed pattern was indeed due to EF-EGPF and LF-EGFP intracellular localization.

It is not the first time bacterial toxins and pathogens have been reported not to traffick through Tfn- and EEA1- containing early endosomes. It has been shown that also cholera toxin B- and Simian virus 40-containing organelles are distinct from classical EEA1- and Tfn- positive endosomes, but communicate with early endosomes via a pathway regulated by Rab5.

These data show that the endocytosis of EF and LF mediated by the binding of PA to its receptors in BHK-21 cells is efficient and extremely rapid. No remaining EF and LF was detected on the cell surface 10 minutes after toxin addition. The kinetics observed are consistent with the model recently proposed for anthrax toxin entry into cells. That is, upon receptors binding, anthrax toxin trigger its own endocytosis via modifications of the anthrax toxin receptor cytoplasmic domain that occur upon toxin binding, and this in turn is necessary for rapid uptake via endocytic vesicles [30, 109].

Late endosomes

The site wherefrom EF and LF exit the endosomes and enter the cytosol is an important point to address and available data are contradictory.

Since the cytosolic activity of the fluorescent chimeras in cultured cells was observed to appear about 40 minutes after toxin addition (Fig. 2, 3), the same incubation time was chosen to image EF-EGFP and LF-EGPF in the last stage of their trafficking through endosomal pathway by fluorescence microscopy. 40 minutes after PA and EF-EGFP or LF-EGFP addition, both toxins localized within perinuclear late endosomal compartments (Fig. 7), as indicated by the extensive colocalization with the lipid molecule lysobisphosphatidic acid (LBPA). LBPA is considered a specific marker of LEs since it is found exclusively in these organelles and accounts for ~15% of the total late endosomal phospholipids [67].

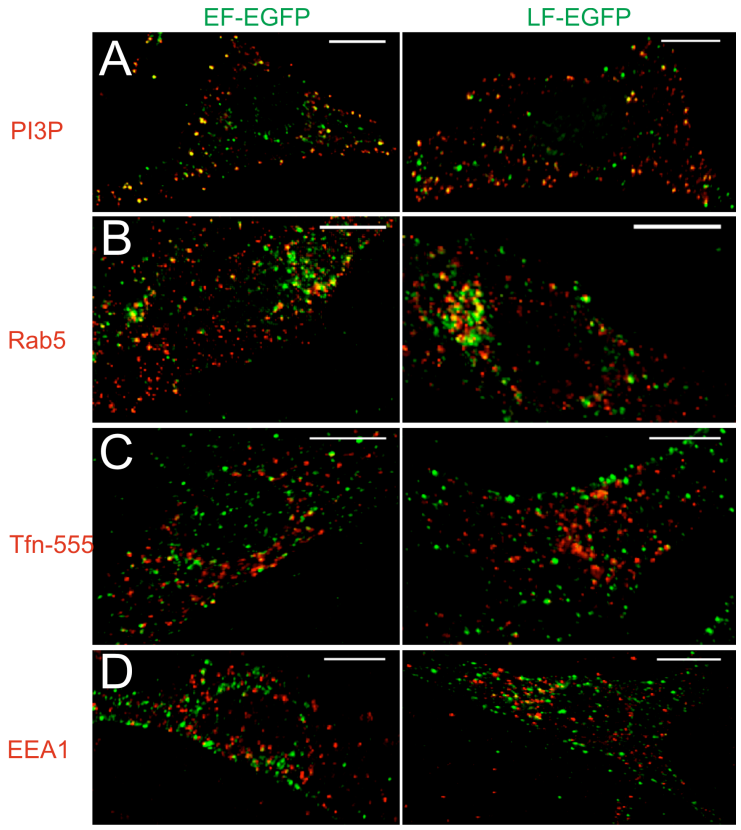

Fig. 6 *Trafficking to early endosomes.* Intracellular distribution of the chimeric toxins in BHK cells treated with PA together with EF-EGFP (left) or LF-EGFP (right) for 10 minutes at 37°C. Cells were stained for PI3P (A), Rab5 (B), Tfn (C) and EEA1 (D). Every image is the 2D maximum intensity projection of z-stack sections after restoration. The overlap between the two signals is depicted in yellow. Scale bar is equal to 10 µm.

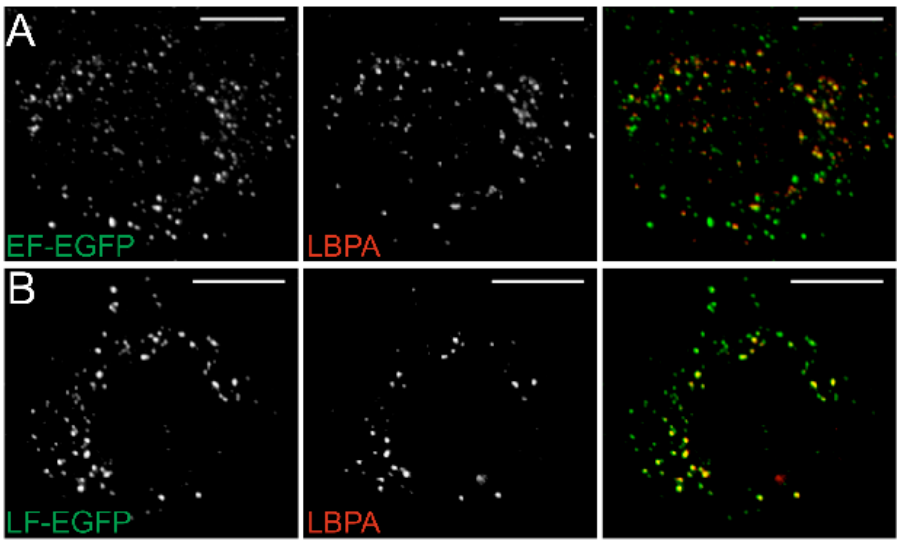

Fig. 7 *Sorting to late endosomes.* Intracellular distribution of EF-EGFP (A) and LF-EGFP(B) after 40 minutes of incubation with PA at 37°C in BHK cells. The samples are fixed for fluorescence microscopy and stained for anti LBPA. On the right the overlap between EGFP (green) and LBPA (red) signals is depicted in yellow. 2D projections of 3D z-stack sections are shown. Scale bar 10 µm.

These data clearly indicate that in BHK-21 cells EF and LF reach late endosomal compartment, wherefrom they translocate into the cytosol.

Our data are consistent with the kinetics reported for EF [80] and LF [79] activity on cellular substrates. Contrarily, other reports suggested that LF reach the cytosol from EEs in RAW264.7 macrophage cell line [81] and Chinese hamster ovary (CHO) cells [79]. This discrepancy can be due to differences in experimental conditions and cellular physiology manipulation, and imaging fluorescent EF and LF chimeras intoxicated cells, in conditions that simulate the *in vivo* situation, is indeed a good tool to address this issue.

Moreover, our data support the kinetics reported for LF on substrates with different intracellular localization. A scaffolding complex that enables the association of MKK1 with LEs was recently identified [110]. It was shown that LF cleaves MKK1 more rapidly than, for example, MKK3 that is not associated to late endosomal membranes. In addition, LF-induced ERK1 inactivation via MKK1 was shown to occur at fivefold lower LF concentrations than p38 inactivation via MKK3 [111], making it likely that LEs act as an encounter platform between LF and its early targets, providing a system of delivery to the perinuclear region. Given the relevance of compartmentalization of intracellular signaling events, EF and LF cytoplasmatic delivery from late endosomes might play a key role on anthrax toxin action on target cells.

2. Anthrax toxin localization after cytoplasmic delivery

In this project, EF and LF intracellular localization after cytoplasmic delivery has been addressed by using different approaches. Cytoplasmic localization of EF-EGFP and LF-EGFP was studied by fuorescence microscopy imaging in cultured cells. Another approach was the development of a FRET-based biosensor to monitor spatiotemporal LF activity in eukaryotic cells and compare it with that of EF. Surface Plasmon Resonance was used to study the interaction between EF and isolated endosomal membranes *in vitro*. Finally, in order to establish which EF domain endows the protein to interact with endosomal membranes, a recombinant EF protein, with the N-terminal domain swapped with that of LF and fuse do EGFP was imaged by fluorescence microscopy in culture cells.

EF-EGFP and LF-EGFP cytoplasmic localization

EF-EGFP and LF-EGFP were imaged by fluorescence microscopy in BHK-21 cultured cells. Fig. 8 shows that 90 minutes after their addition, EF-EGFP and LF-EGFP have different intracellular fluorescence staining pattern reflecting a different cytoplasmic localization. LF-EGFP is clearly cytosolic, though its fluorescence signal is weak, a fact that is expected because the signal is dispersed in a large volume. Despite the low fluorescence signal of LF, its distribution is not exactly homogeneous throughout the cytoplasm, as it appears to be more concentrated on cellular organelles. This interpretation is in agreement with the fact that LF is active on MKK isoforms that are reported to localize on organelles. (e.g. MKK1-2 on Golgi and endosomes, MKK6 on mitochondria). Conversely, EF-EGFP appears in a spotty and perinuclear fluorescence distribution and shows an extensive colocalization with the LBPA-specific marker of LEs.

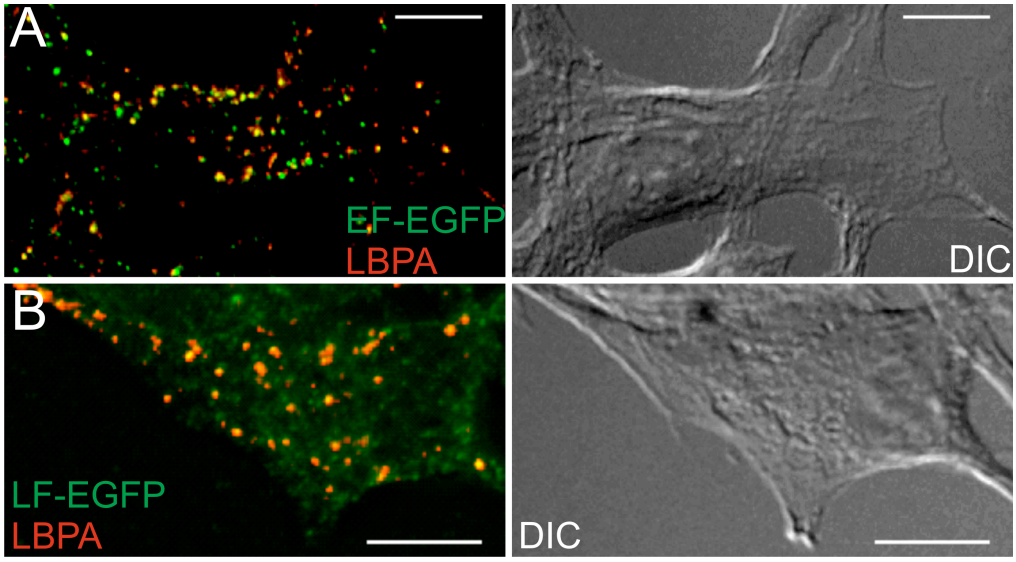

Fig. 8 *Intracellular localization after translocation from (PA63)7 pore.* Intracellular distribution of BHK cells incubated with PA and EF-EGFP (A) or LF-EGFP (B) at 37°C for 90, fixed and immunostained with appropriate antibodies. DIC images and merged 2D channels, after restoration of a 3D stacks, are shown. Scale bar, 10 µm.

Together with the fact that, 90 minutes after addition, EF-EGFP has translocated across the late endosomal membranes and has already caused a large increase in cAMP intracellular concentration (Fig. 2), this observations clearly indicate that *in vivo* EF translocates from the lumen of LEs to the cytosol and stays associated to the cytosolic surface of these intracellular compartments, wherefrom it exerts its adenylate cyclase activity. EF would become a novel enzyme on the cytosolic surface of LEs, across the cytosol, with the possibility of generating cAMP gradients across the cytoplasm, from the perinuclear area to the cortical sub-plasma membrane region, and this indeed is the case [80].

Scaffolding proteins such as A kinase-anchoring proteins (AKAPs) have been shown to be responsible for the compartmentalization of adenylate cyclases and cAMP effectors, suggesting that cAMP signaling events are both temporally and spatially restricted [112]. Taken together, these observations suggest that compartmentalization of EF action might be crucial to specific cAMP-dependent actions during *B. anthracis* infection.

FRET-based LF activity biosensor

Since EF and LF exert their activities in the target cell cytosol, studying *in vivo* the spatiotemporal dynamics of EF and LF activity in single cell can give very useful information on their localization after cytoplasmic delivery.

Available data on the spatiotemporal dynamics of EF activity in HeLa cells, using a FRET-based cAMP reporter, showed a peculiar sustained activity in the perinuclear area (where LEs concentrate) compared to cell periphery [80]. We attempted to design a FRET-based biosensor to monitor by LF activity in space and time and compare its dynamics with those reported for EF [80].

A FRET-based reporter for LF was recently designed in order to screen for LF inhibitors in bacterial systems. A consensus LF recognition sequence is flanked by a FRET pair of optimized fluorescent proteins: a cyan fluorescent protein (CyPet) and a yellow fluorescent protein (YPet). When expressed in *E. coli* cells, the fluorescent LF sensor was reported to show high levels of FRET *in vivo* in the absence of LF. Conversely, when LF and its FRET-based substrate were expressed sequentially in the same bacterial cell, the FRET signal was significantly reduced [113]. In the presence of LF, the consensus recognition sequence is cleaved, resulting in the release of the two fluorescence proteins that diffuse apart thus lowering FRET (Fig. 9, left).

The FRET-based reporter described above was cloned in the mammalian cell vector pcDNA3.1. When over-expressed in transfected HeLa cells, the LF reporter was evenly distributed in the cell cytosol (Fig. 9, right).

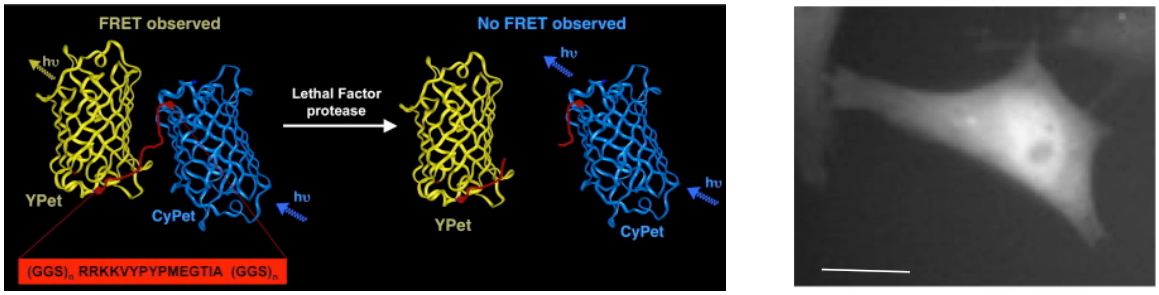

Fig. 9 *FRET-based LF reporter.* A scheme of the FRET reporter used is shown (left). In red, single letter codes represent LF recognition sequence and linkers. (Right) Live cell fluorescence imaging of HeLa cells overexpressing the FRET-based LF reporter. Scale bar 10 µm.

Fig. 10A shows a time course of the fluorescence emission ratio changes recorded in transfected HeLa cells exposed to PA and LF at time zero. The time course of the FRET changes were monitored in different intracellular domains in order to have a spatiotemporal resolution. However, the increase in the emission ratio starts from the moment of toxin addition and the signal is more likely to represent a drift rather than the specifically due to LF activity. Moreover, a sustained increase in the emission ratio should be recorded not before 40 minutes after toxin addition, which was the case of the FRET-based EF biosenor [80], as EF and LF need to be trafficked to LEs and are active in the cytosol 40 minutes after toxin treatment (Fig. 2 and 3). Therefore, as a control, changes in LF reporter fluorescence emission ratio were monitored in HeLa cells exposed only to PA (Fig. 10, lower panel). The trend recorded was the same observed in the case of addition of LF and PA (Fig. 10, upper panel), indicating the signal recorded is not due to LF activity.

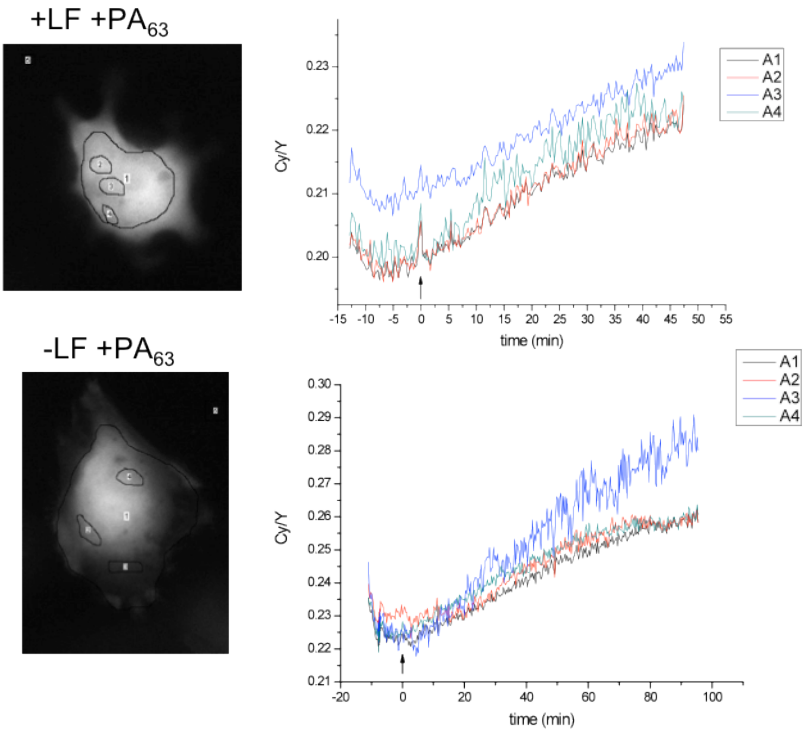

Fig. 10 *FRET analysis of LF activity in cultured cells*
HeLa cells expressing the FRET-based LF reporter were treated with the anthrax toxin active subunit LF in presence (upper) and in absence (lower) of the binding subunit PA (arrowhead at time 0) and were maintained at 37°C during microscopic observations. CFP/YFP ratios were measured in the indicated areas (1-4).

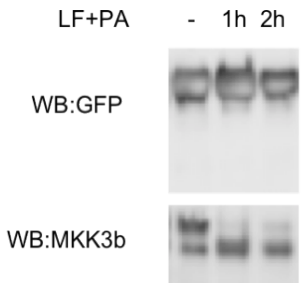

Fig. 11 *FRET analysis of LF activity in cultured cells*
HeLa cells expressing the LF reporter were treated with LF+PA_{63} for 1h or 2h at 37°C or left untreated. Total cell extracts were separated by SDS-PAGE, blotted onto nitro-cellulose paper and stained with anti-GFP and anti-MKK3 antibodies.

To test LF activity on the cAMP FRET sensor, HeLa cells were transfected with the reporter, exposed to LF and PA for 1 or 2 hours and subsequently lysed. Total cell lysates were separated by electrophoresis, blotted, and the reporter was revealed with anti GFP antibody. Fig. 11 shows that a high amount of LF reporter was present in transfected in HeLa cells but it was not cleaved upon 1 and 2 hours of LeTx treatment. This is not the case of MKK3b, one of the physiological substrates of LF, which is efficiently cleaved by the toxin in these cells, indicating LF is active but not on the FRET-based reporter.

In this experiment we used the same coding sequence for LF reporter that have been used by Kimura and colleagues in a bacterial system. Assuming that the protein encoded by this construct has the same functionality in both procariotic and eukaryotic cells, a possible explanation for this negative result is the inadequate ratio between LF and the FRET-based substrate reached in LeTx treated cells. LeTx enters the target cell upon receptor binding and trafficking along the endocytic pathway, therefore the amount of LF molecules delivered to the cytosol is likely to be lower compared the amount reached when over-expressed in cells in Kimura et al. system. The low LF : FRET-based reporter ratio may account for this negative result.

It should be also taken into account that kinetics and mechanisms that take efficiently place in a bacterial system, may not be the same in the more complex eukaryotic system, in the presence of the physiological substrates of the toxin. In fact, although LF cleaves MKKs on a consensus sequence located outside their catalytic domain, another LF interacting region essential for LF-mediated cleavage was recently identified within the C-terminal kinase domain of MKK1 [87, 88]. These findings support the idea that in the system used, LF reporter competes with the cellular full-length MKKs, which may have a higher affinity for the toxin.

EF interaction with endosomal membranes in vitro

The interaction between EF and endosomal membranes isolated from BHK-21 cells was analyzed here by Surface Plasmon Resonance (SPR) with a BIAcore instrument.

SPR has become one of the most important label-free technologies for analyzing macromolecular interactions. Biomolecular interactions are studied at the surface of so-called “sensor chips”, glass

slides coated with a thin layer of gold on one side while on the opposite side there is a matrix designed for biological interactions. The phenomenon of Surface Plasmon Resonance occurs in condition of total internal reflection by thin layers of certain metals. A polarized light is directed to the thin layer of gold which lies on one side of the sensor chip (Fig. 12). At a critical angle of incident light plasmons are generated at the surface of the gold layer thus generating a decrease in the intensity of reflected light. The critical angle is dependant upon changes in the refractive index of the matrix within a few hundred of nm of the surface and it changes when molecules interacts to the surface, associating or dissociating. In the Biacore system we used, one substance, termed the *ligand*, is attached on the surface of a sensor chip. The second one, termed *analyte*, is then pumped across the surface via a microfluoidic system. If the interaction between the ligand and the analyte occurs, the refractive index at the surface of the chip changes and it is viewed as increase of signal. The Biacore system records the response as resonance units (RU) (equal to a critical angle shift of 10^{-4} deg), describing the increase of the signal. There is a linear relationship between the mass of the matter at the surface of the chip and the RU, therefore SPR can give a measure of the mass concentration at the surface of the chip. SPR is widely used to study protein-protein interactions but recent developments enable its use for the analysis of membrane-protein interactions.

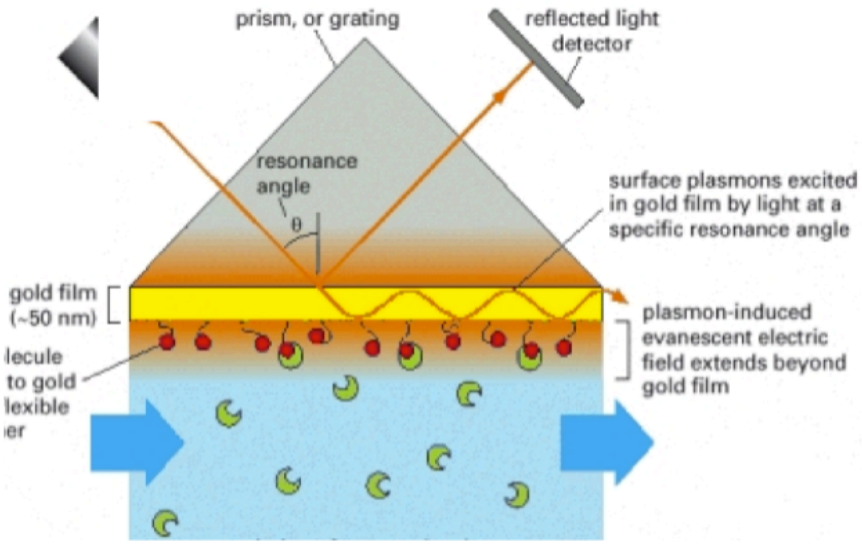

Fig. 12 *Surface Plasmon Resonance*

In our case, we preferred to study EF interaction with isolated late endosomal membranes rather than artificial membranes to ensure the biological composition and ratio between the components would reflect the *in vivo* situation. Moreover, this approach can lead to the identification and isolation of EF binding partner on endosomal membranes.

Late endosomes were prepared using a well-established cell fractionation protocol [57, 72]. Ultracentrifugation of BHK-21 cells homogenate gave a organelle-free postnuclear supernatant (PNS) and a organelle-containing suspension, which was then further fractionated on a sucrose density gradient into a LEs membrane (enriched in LAMP2), EEs membrane (enriched in EEA1) and a heavy membrane (HM) fraction, the latter comprised of all the other cellular membranes (e.g. Golgi, plasma membrane, endoplasmic reticulum and mitochondrial membranes) (Fig. 13)

LEs, EEs and HM as control were adsorbed on different parallel flow cells of a HPA Biacore sensor chip. The flat hydrophobic surface of the HPA chip, consisting of long-chain alkanethiol molecules, facilitates the adsorption of lipid monolayers. The three isolated membrane fractions were well-adsorbed and all of them saturated the hydrophobic surface of their flow cell (data not shown), therefore it can be assumed the three flow cells are coated with an equal amount of membranes.

Upon EF injection, the flow cell coated with late endosomal membranes recorded a higher RU response, compared to the ones coated with early endosomal and heavy membranes (Fig.14A), indicating the interaction between EF and late endosomal membranes occurs in this *in vitro* model membrane system. Conversely, injected bovine serum albumine (BSA) gives no response to any of the membranes tested, indicating the specificity of the interaction observed (Fig.14B).

EF slightly interacts also with both EEs and HMs, although the signal recorded is lower than the one reported for LEs. However, based on the presented data, we cannot rule out a possible binding between EF and EEs and other cellular membranes. However, assuming the three flow cells were coated with equal amounts of membranes, it is more likely that the EF weak interaction reported with EEs and HMs is due to contamination during cellular fractioning rather than a specific binding to these compartments. Moreover, it should be recalled that, even though different endosomal compartments are easily distinguishable due to their characteristic size and molecular composition, the boundaries between different compartments of the same pathway are not so well defined on the molecular level. In this view, an alternative explanation for the weak signal observed on EE and HM could be that the endosomal components which interact with EF are be enriched in LEs (representing the toxin site of exit from the endosomal pathway) but present also, in a lesser extent, in EEs and other cellular membranes. Taken together, these data confirm that EF endosomal localization after cytoplasmic delivery is due to the interaction between EF and late endosomal membranes.

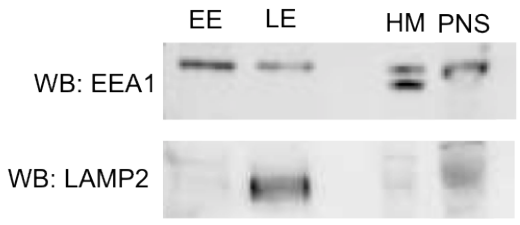

Fig. 13 *Endosomal membranes isolation*
BHK cells were lysed and the postnuclear supernatant (PNS) was isolated and fractionated on a sucrose density gradient, resulting in three fractions: early endosomes (EE), late endosomes (LE) and heavy membranes (HM). 10 µg of each fraction, including the PNS input, were subjected to SDS-PAGE and immunoblotted with antibodies

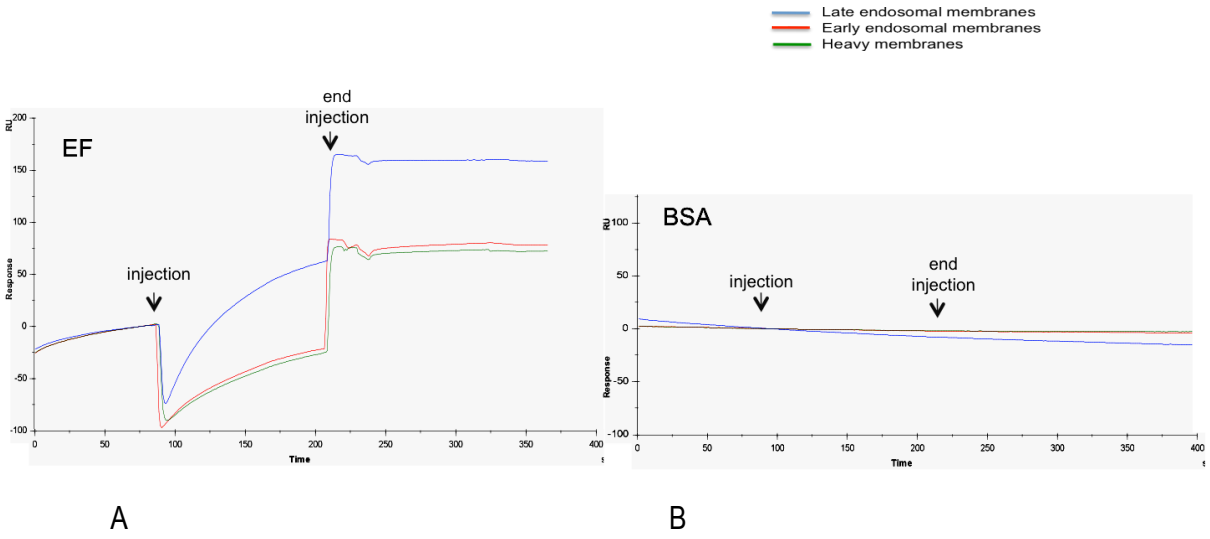

Fig. 14 *EF interaction with isolated endosomal membranes* Isolated EE (red plot), LE (blue plot) and HM (green plot) were adsorbed on a HPA sensor chip. Injections of (A) EF (50 µg/ml) or (B) BSA (100 µg/ml) were made onto the surface of the membranes (arrowheads), and their binding was recorded in real time by Surface Plasmon Resonance using a Biacore 3000 system.

Endocytic compartments, especially LEs, are known to contain a high amount of invaginated membranes and intraluminal vesicles, which do not face the cytosol. Moreover, intralumInal and limiting membranes on the same endocytic compartment have been shown to consist of different membrane microdomains with different biophysical properties [57]. These domains consist of specialized protein-lipid combinations, or of protein complexes associated with specific membrane lipids. In our experiments, the injected biological membranes are adsorbed by the hydrophobic HPA sensor chip and result in the formation of a lipid monolayer. This, in turn, results in the exposure to the *analyte* of the cytosolic leaflet, but also of the luminal leaflet and the high amount of intralumenal invaginations of the biological membrane tested, which obviously cannot be targeted by EF after cytoplasmic delivery. Indeed, the signal observed for the interaction between EF and late endosomal membranes adsorbed on HPA chip is not very high.

In order to optimize the response, further experiments will be done using the recently developed sensor chip L1. This chip is composed of lipophilc groups covalently attached to the dextran matrix, making the surface suitable for direct attachment of entire endosomal vesicle, resulting in the exposure exclusively of the cytosolic side of endosomal membranes to the *analyte*.

Role of EF N-terminal domain in endosomal membrane interaction

In order to establish which domain of EF is involved in localization on late endosomal membranes, we used a domain swap approach.

The crystal structures of EF and LF showed that the PA-binding N-terminal domain of both proteins, termed EF_N and LF_N respectively, correspond to discrete folding domains of the parent proteins and are loosely tethered to the C-terminal, multidomain catalytic regions. EF_N and LF_N share 35% sequence identity and similar structural architecture and they share crucial functions for the entry and cytoplasmic delivery of EF and LF [2, 22]. However, the overall structure of these two domains differs significantly, with the major difference lying in five surface exposed joining loops L1-L5, which might account for EF and LF different cytoplasmic localization.

To test whether the N-terminal EF domain is necessary for the interaction with late endosomal membranes, chimeric EF and LF with swapped PA-binding N-terminal domains were fused to fluorescent proteins and imaged by fluorescence microscopy in cultured cells. The main reason we chose this approach as opposed to a deletion mutagenesis strategy is that EF_N and LF_N domains are essential for binding to PA at the cell surface and for membrane translocation. Moreover, it has been reported that LF_N can be fused to a variety of other proteins, such as shiga toxin A or diphteria toxin A fragment (DTA), and can mediate their cytosolic delivery in the presence of PA [51, 52].

Design, expression and purification of swapped N-terminal EF and LF fluorescent chimeras

N-terminal domain swapped EF and LF were fused on the C-terminal to the fluorescent proteins EGFP and mCherry, respectively, generating the mutants LF_NEF-EGFP and EF_NLF-mCherry.

LF_N (residues 1-253) and EF_N (residues 1-254) were cloned into pRSET A (Invitrogen) plasmids, upstream the sequence coding for the three catalytic domains of EF and LF, respectively, which were amplified by PCR from their full-length sequences. Finally, EGFP and mCherry coding sequences were subcloned downstream the swapped LF_NEF and EF_NLF constructs, respectively, as depicted in Fig. 15.

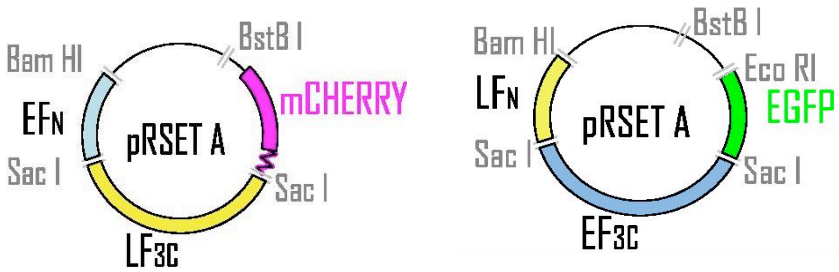

Fig. 15 *Schematic representation of N-terminal swapped fluorescent chimeras.* EF_NLF-mCherry (left) and LF_NEF-EGPF (right)

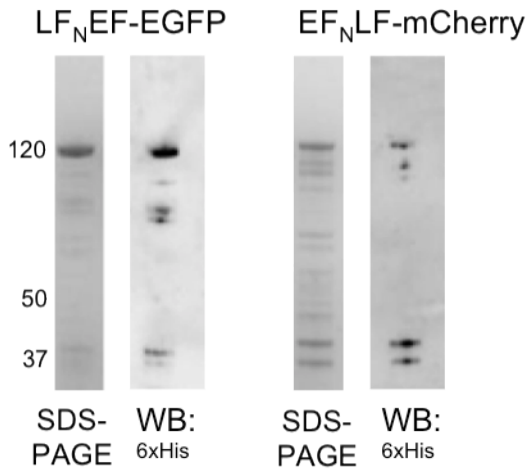

Fig. 16 *SDS-PAGE and immunoblot analysis of LFNEF-EGFP and EFNLF-mCherry.*
LF_NEF-EGPF and EF_NLF-mCherry (0.1 µg) were separated by SDS-PAGE and immunoblotted using anti 6xHis antibodies.

The plasmids containing the swapped chimeras were introduced into *E. coli* BL21 pLysS cells and the proteins were induced to over-express by IPTG addition. The expression was maximized after 4 hours of induction at 30°C. The recombinant LF_NEF-EGFP and EF_NLF-mCherry have a 6xHis tag on the N-terminal which allows purification by affinity chromatography and was shown to confer LF an increased capacity of entering and translocating across the $(PA63)_7$ transmembrane channel [49].

The purified LF_NEF-EGFP migrated mostly as a single band (~120 kDa) on SDS-PAGE, while EF_NLF-mCherry migrated as multiple bands, reflecting higher protein contamination (Fig. 16). Both LF_NEF-EGFP and EF_NLF-mCherry were reactive to anti- 6xHis antibody by western blot.

EF_NLF-mCherry in vitro characterization

EF_NLF-mCherry activity was tested by *in vitro* incubation with one of LF substrates, MKK6, fused with the bulky GST moiety at the N-terminus (referred to as GST-MKK6). Since LF targets a unique site of cleavage (between residues 14-15) on the N-terminal region of MKK6 [114], the N-terminal GST fusion allowed the detection of the cleaved substrate by SDS-PAGE.

Fig. 17A shows that chimera was active, as after 3 hours of incubation with GST-MKK6, followed by SDS-PAGE migration, a decrease in the band intensity of GST-MKK6 (~64 kDa) and the appearance of two easily distinguishable bands, were observed (arrowheads). The first band (~28 kDa) corresponds the GST fused to the 14 N-terminal MKK6 residues (GST-$MKK6_{1-14}$) and the second, with lower electrophoretic mobility (~36 kDa), corresponds to MKK6 lacking the first 14 residues ($MKK6_{\Delta 1-14}$). This result indicates that swapping N-terminal domain and fusing mCherry on the C-terminal, do not affect LF catalytic activity *in vitro*.

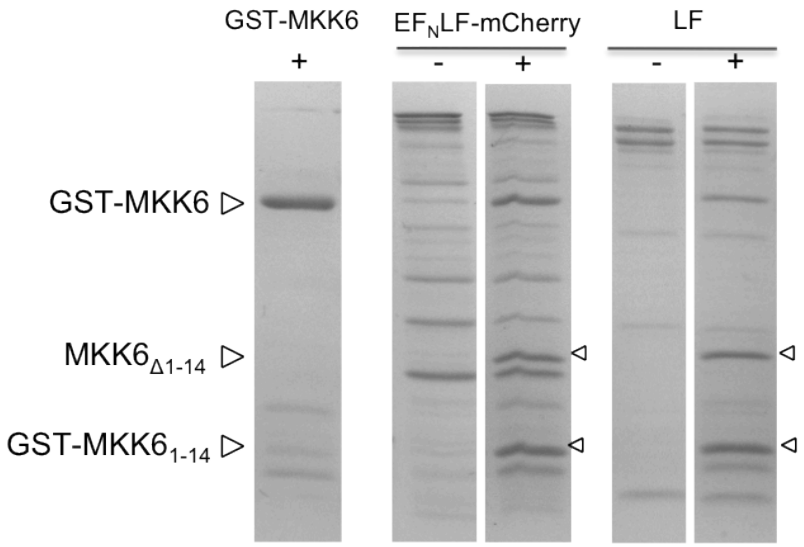

Fig. 16 *EF$_N$LF-mCherry activity in vitro.* Endopeptidase activity of EF$_N$LF-mCherry was tested *in vitro*, on the basis of its ability to cleave the bulk of the GST sequence from the N-terminus of MKK6. EF$_N$LF-mCherry or LF were incubated with GST-MKK6 (enzyme:substrate molar ratio 1:5) for 3 hours at 37°C. The reaction products were separated by SDS-PAGE, gels were stained with Coomassie Blue. Arrowheads indicate the two fragments resulted from GST-MKK6 cleavage.

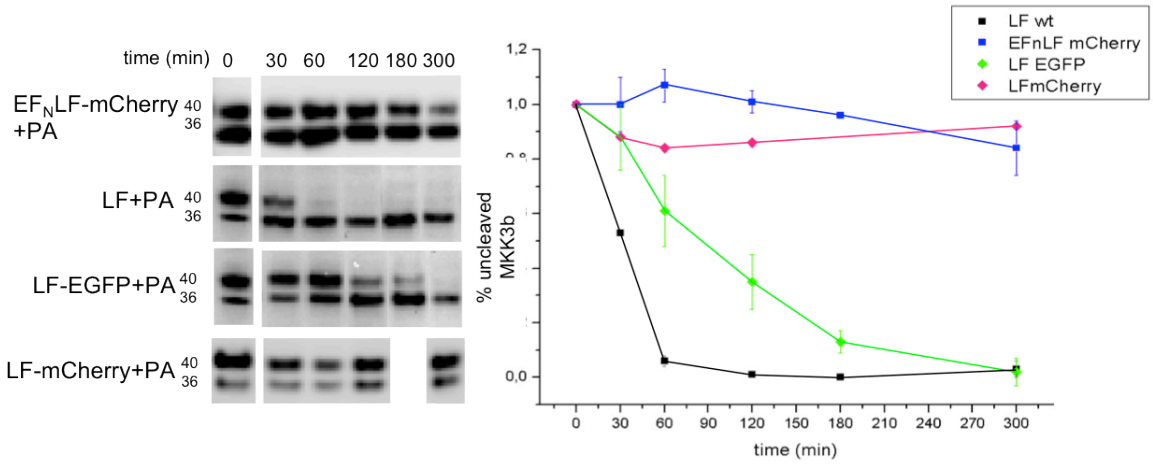

Fig. 17 *EF$_N$LF-mCherry activity in cultured cells.* Time course of MKK3b cleavage in BHK cells incubated with PA and EF$_N$LF-EGPF, or LF, or LF-EGFP, or LF-mCherry. Total cell extract were separated by SDS-PAGE and immunoblotted with an anti-MKK3 antibody (left). The densitometric quantification of the bands was expressed as the ratio between the MKK3b bands and the lower molecular weight band intensities, and was normalized against the control (right).

EF_NLF-mCherry activity in cultured cells

Unfortunately, at the moment of this swapped chimeras study, we still had not gained the knowledge that proteins fused to mCherry lose their ability to translocate across PA channel, resulting in the unsuccessful delivery to the cell cytosol.

To test the functionality of the fluorescent domain swapped LF chimera, the time course of MKK3b cleavage in BHK-21 cells treated with PA and LF or EF_NLF-mCherry or LF-EGFP or LF-mCherry was observed. Total cell extracts were made at given time, separated by SDS-PAGE, blotted and stained with anti MKK3 antibodies, as previously described (Fig. 17, left). The percentage of cleavage over time was quantified and normalized to the control (Fig. 17, right). As expected, EF_NLF-mCherry was not active in the cell cytosol and the same result was observed for LF-mCherry. Conversely, LF and LF-EGFP were active, even though with slightly different kinetics, as it was previously observed.

This data, support the finding that mCherry derivatives do not translocate across PA channel on endosomal membranes, due to a higher resistance to unfolding than EGFP, as previously described. Therefore the N-terminal domain swapped LF could not be imaged in host cell cytosol by fluorescence microscopy.

LF_NEF-EGFP intracellular localization

LF_NEF-EGFP was imaged by fluorescence microscopy in BHK-21 cultured cells 90 minutes after addition in presence of PA. In Fig. 18, the swapped chimera was clearly localized on late endosomes, as the fluorescent staining extensively colocalized with the LBPA specific marker in the perinuclear area of the cell.

The chimera had not been characterized yet, but we assume that, swapped domain N-terminal with LF and fused EGFP would not affect the entry and trafficking pathway seen for both EF-EGFP and LF-EGFP, and which was shown to be identical. 90 minutes after addition, the swapped LF_NEF-EGFP had clearly the same intracellular distribution as the one reported for the full length EF-EGFP, rather than the weak cytosolic signal reported for LF-EGFP at this time point.

Taken together, these observations rule out the possibility that EF N-terminal domain is responsible for the protein interaction with endosomal membranes after cytoplasmic translocation. However, these data need to be confirmed by designing and imaging the swapped LF conunterpart fused to EGFP, which should disperse in the cytosol as it was shown for LF-EGFP.

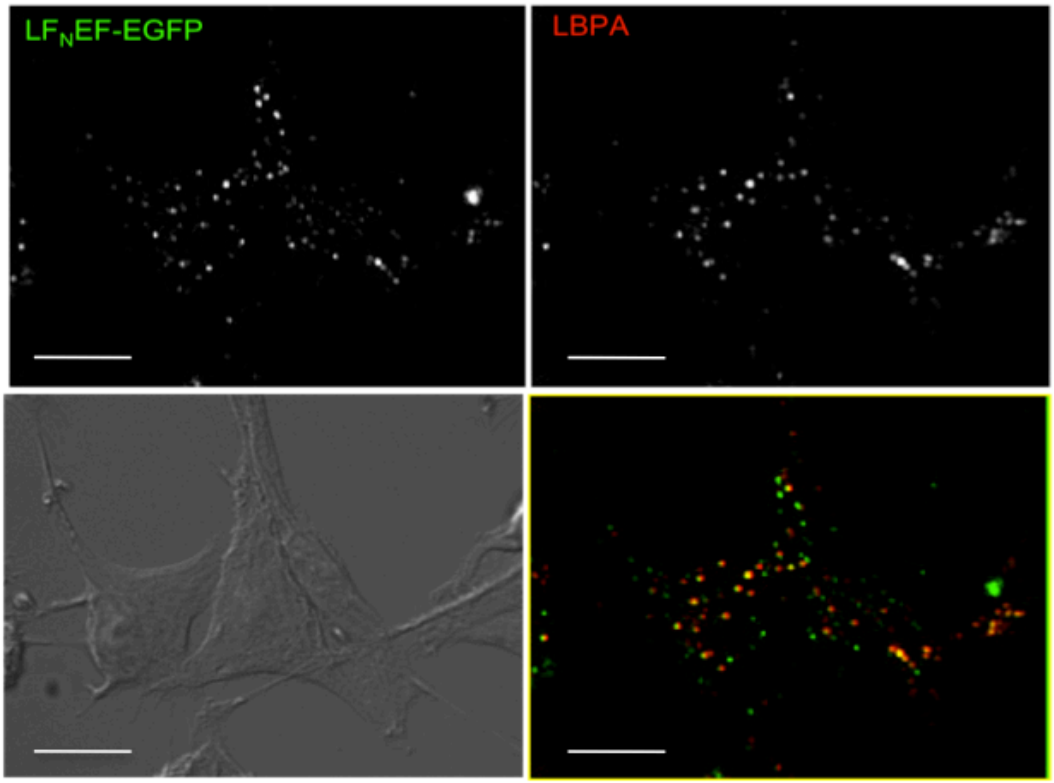

Fig. 18 *LF$_N$EF-EGFP Intracellular localization upon translocation across (PA$_{63}$)$_7$ channel.* Intracellular distribution of BHK-21 cells incubated with PA and LF$_N$EF-EGFP at 37°C for 90, fixed and immunostained with anti-LBPA antibodies. DIC image and 2D projections of z-stack sections are shown. The overlap between LF$_N$EF-EGFP (green) and LBPA (red) signals, is depicted in yellow (bottom right). Scale bar 10 µm.

Materials and Methods

Cells, antibodies and reagents

BHK-21 cells and HeLa cells were maintained in DMEM (Gibco) supplemented with 10% heat-inactivated foetal calf serum (FCS, Euroclone), penicillin (100 U ml^{-1}) and streptomycin (100 U ml^{-1}). Antibodies were obtained from the following sources: anti-His tag monoclonal antibody from Novagen, monoclonal antibodies anti-GFP and anti-6xHis from Abcam, anti-EEA1 antibody from BD Transduction Laboratories, anti-PI3P from Echelon, anti-Rab5 from Synaptic System, anti-MKK3 from Santa Cruz Biotechnology, anti-LBPA (6C4) was a kind gift of J. Gruenberg (University of Geneva, CH), Tfn-Alexa555 and fluorescently labeled secondary antibodies from Molecular Probes; FuGENE HD from Roche Diagnostics Corporation. Reagents were Sigma-Aldrich and Calbiochem.

FRET imaging of cAMP intracellular dynamics

BHK cells (2 10^5) were co-transfected reagent with 1 μg of two pcDNA3.1 plasmids, one carrying the catalytic (C) subunit of PKA fused to YFP (C-YFP) and one carrying the regulatory (R) subunit of PKA fused to CFP (RII-CFP) [115] using Fugene HD, following manufacturer's instructions. 48 hours after transfection, cells were incubated in a balanced salt solution (NaCl 135 mM, KCl 5 mM, KH2PO4 0.4 mM, MgSO4 1 mM, HEPES 20 mM, CaCl2 1.8 mM, glucose 5.4 mM, pH 7.4) in a microscope-adapted micro-incubator equipped with a temperature controller (HTC, Italy) at 37°C and constant 5% CO2 pressure. PA (400 nM) and EF (200 nM) or EF-EGFP (200 nM) or EF-mCherry (200 nM) were added after about 15 min of imaging, and images were recorded every 20 sec for the indicated time periods. Integration time was 200 ms. At the end each eperiment forskolin (Frsk) (25 μM) was added as internal control. At each time point, the intracellular cAMP level was estimated by measuring the ratio between the background-subtracted CFP emission image and the YFP emission image upon excitation of CFP (R CFP/YFP) [116]. Images were acquired using an oil immersion 40X PlanApo 1.4 NA objective on a Leica DMI6000 microscope.

FRET images were collected through a BP 436/20-nm excitation filter and a custom-made optical beam splitter built with a 515 nm dichroic mirror and ET 480/40-nm and ET 535/30-nm emission filters. A cooled camera from OES (Padova, Italy) with a 1,4 Megapixel CCD and a sensor resolution of 1360 X 1024 Pixels was used. The acquisition software was from OES (Padova, Italy). Recorded images were processed with WCIF ImageJ v1.40 (http://rsb.info.nih.gov/ij).

Cloning FRET-based LF biosensor

The coding sequence for LF cleavage site flanked by five GGS repeats linkers ($(GGS)_5$-RRKKVYPYPMEGITA-$(GGS)_5$) and C-terminally fused to yellow fluorescent protein (LFp-YPet) was obtained from the plasmid Pet28a3 [113], digested with BamHI and XhoI restriction enzymes and inserted in pcDNA3.1 (Invitrogen). Cyan fluorescent protein (CyPet) was PCR-amplified from pCyPet-His (Addgene) using the following primers: forward 5'- AAA GGT ACC ATG GCT AAA GGT GAA GAA TTA TTC GGC -3' and reverse 5'- AAA GGA TCC TTT GTA CAA TTC ATC CAT ACC ATG GGT -3'. On the forward primer, downstream the starting codon a thymine (T) was substituted with a guanine (G) to follow the Kozak consensus sequence for protein for protein translation in eukaryotic systems. CyPet fragment was digested with BamHI and KpnI and inserted in pRSET A (Invitrogen) upstream the sequence coding for LFp-Ypet. The sequence of the FRET-based LF biosensor (YPet-LFp-CyPet) was confirmed by DNA sequencing.

FRET imaging of LF dynamics

BHK cells were transfected with 1 μg of pcDNA3.1 plasmid carrying the consensus LF cleavage sequence flanked by a FRET pair of optimized fluorescent proteins: cyan fluorescent protein (CyPet) and yellow fluorescent protein (YPet) using FugeneHD, following manufacturer's instructions. 48 hours after transfection, cells were incubated in a balanced salt solution (NaCl 135 mM, KCl 5 mM, KH2PO4 0.4 mM, MgSO4 1 mM, HEPES 20 mM, CaCl2 1.8 mM, glucose 5.4 mM, pH 7.4) in a microscope-adapted micro-incubator equipped with a temperature controller (HTC, Italy) at 37°C and constant 5% CO2 pressure. PA (400 nM) with or without LF (200 nM) was added after about 15 min of imaging, and images were recorded for the indicated time periods every 20 sec. Integration time was 200 ms. At each time point, the FRET sensor cleavage was estimated by measuring the ratio between the background-subtracted CFP emission image and the YFP emission image upon excitation of CFP (R CFP/YFP). The microscope, excitation and emission filters, digital camera and acquisition software used were previously described.

MEK3 cleavage by chimeric lethal factor

BHK cells (1.5×10^4) were incubated with PA_{83} (400 nM) and LF (200 nM) or LF-EGFP (200 nM) or

LF-mCherry (200 nM) or LF_NEF-EGFP (200 nM) in DMEM 1% w/v BSA at 37°C for different incubation times in a 96-well plate. After the removal of the culture medium, the cells were lysed, separated on SDS-PAGE, and immunoblotted with anti-MKK3 antibodies. The membranes were developed using ECL plus detection system (Amersham Biosciences), and chemiluminescence emission was detected with ChemiDoc™ XRS (Biorad). The antibody identifies two splicing isoforms of MEK3, MEK3b and MEK3a, a variant lacking of the first 29 residues. Only MEK3b is cleaved by LF and the cleavage percentages were quantified considering the ratio between each MEK3b band and the band intensity at lower molecular weight, and the results was normalized against the control. Band intensities were quantified with Quantity One software from Biorad.

Translocation of chimeric proteins across artificial membranes

Planar phospholipid bilayers were formed by standard methods [117]. Once a membrane was formed, PA_{63} prepore (25 pM) was added to the *cis* compartment, held at a $\Delta\Psi$ = +20 mV with respect to the *trans* compartment. Free PA_{63} not inserted into the membrane was removed by perfusion. Binding cargo (LF, EF, or chimeric proteins) was added to the *cis* compartment (1 mg ml^{-1}), and the progress of binding to PA channels was monitored by the decrease in conductance. Translocation was initiated by raising the pH of the *trans* compartment to pH 7.2 with 2 M KOH, while maintaining the *cis* compartment pH at 5.5. At the same time, the membrane potential was increased from $\Delta\Psi$ = +20 mV to $\Delta\Psi$ = +50 mV. Experiments were normalized to controls lacking cargo protein (*n*=3). All planar phospholipid experiments were performed in a Warner Instruments Planar Lipid Bilayer Workstation (BC 525D, Hamden, CT). These experiments were performed in collaboration with Blythe Janowiak and R. John Collier, Department of Microbiology and Molecular Genetics, Harvard Medical School, Boston, USA.

EGFP and mCherry guanidine hydrochloride-induced equilibrium unfolding .

Protein samples (0.050 mg ml^{-1} in 50 mM TRIS, pH 8.0) were incubated for 20 hours at 25°C in the presence of various concentrations of guanidine hydrochloride (GndHCl). Unfolding curves were determined by exciting the samples at 365 nm and detecting the emitted fluorescence at 510 nm for EGFP and at 610 nm for mCherry. Fluorescence was recorded in a quartz-microcuvette cell (105.250-QS, Hellma, Milan) kept at 25°C on a Perkin–Elmer LS-50 spectrofluorimeter. The data were analyzed using Origin v. 7.5 software.

Fluorescence microscopy

Sub-confluent BHK cells grown on glass coverslips were rinsed two times with DMEM 2% w/v BSA and treated for different incubation times with and PA_{83} (600 nM) and EF-EGFP or LF-EGFP or LF_NEF-EGFP (200 nM). Cells were then washed with PBS, fixed with ice-cold acetone for 5 min at room

temperature and sequentially incubated with a mixture of primary antibodies and a mixture of fluorophores conjugated secondary antibodies. To monitor cell surface binding, cells were first treated with PA_{83} for 12 min, washed with PBS, incubated with LF or EF derivatives for 2 min at 37°C and immediately washed and fixed. All antibody incubations were performed for 1 h at room temperature. Images were acquired sequentially with a FITC and Texas Red filter sets (Chroma Technology corp., USA) with 250 ms or longer integration times by using an oil immersion 63X PlanApo 1.40 NA objective on a Leica DMIRE3 wide-field inverted microscope, equipped with a DC 500 digital camera from Leica, with a sensor resolution of 1300 X 1030 Pixels. The acquisition software was FW4000 (Leica). Images were processed with ImageJ v1.40 (http://rsb.info.nih.gov/ij)

Endosome preparation by gradient fractionation

BHK cells grown on Petri dishes were washed with ice-cold PBS and scraped in PBS with the addition of Protease Inhibitors Cocktail (Roche). Cells were lysed by passage through a 22-gauge needle in 600 µl of Homogenization Buffer (HB; 8.5% sucrose, 3 mM imidazole, pH 7.4) with the addition of Protease Inhibitors Cocktail (Roche) [72]. The lysed cell suspension was centrifuged, the pellet was discarded, 50 µl of the supernatant were diluted in HB 1:4 and ultracentrifuged at 80 000 r.p.m. for 30 min using a Beckman XL-100 ultracentrifuge (TLA-120.1 Beckman rotor) to obtain a clear postnuclear supernatant (PNS) fraction. PNS was adjusted to 40.6% sucrose, loaded at the bottom of an SW55 tube, and overlaid sequentially with 35% and 25% sucrose solutions in 3 mM imidazole, pH 7.4, and then HB as previously described [69]. The gradient was centrifuged for 60 min at 35 000 r.p.m., using a SW55 rotor. Late endosomal fractions (LE) were collected at the 25%/HB interface, EE at the 35/25% and the HM at the 40.6/35% interface. PNS fractions were collected from the clear, ultracentrifuged PNS, obtained as described above. The proteins content in each fraction was quantified with Bradford assay (Biorad) as described elsewhere (Simpson and Sonne, 1982). 5.5 µg of proteins from each fraction were subjected to SDS–PAGE and analyzed by Western blot.

BIAcore SPR analysis of EF interaction with endosomal membranes

All experiments were performed on a BIAT100 (GE Healthcare) using BIAT100 control software version 1.1.1 and BIAT100 Evaluation Software version 1.1.1 for sensorgram analysis. EF-membranes interaction assays were performed on isolated endosomal membranes prepared from BHK-21 fibroblast cell line as described above. HPA sensor chips (GE Healthcare) were prepared for membrane immobilization following the manufacturer's instructions. BHK isolated late endosomes (LE), early endosomes (EE) and heavy membranes (HM) diluted 1:2 (final concentration 5 µg ml^{-1} total proteins) in HBS-N Buffer (Hepes 10mM, NaCl 150mM, EDTA 3mM pH7.4) were injected for 30 min at a flow rate of 2 µl min^{-1} at 25°C in three parallel flow cells of the sensor chip. Each immobilization was followed by a

short pulse of 10 mM NaOH at the flow rate of 10 µl min^{-1} to remove membrane aggregates and loosely bound structures. The responses recorded after membrane adsorption were 3700, 4000, 3800 resonance units (RU) for EE, LE and HM, respectively. HBS-N Buffer pH7.4was used as running buffer. For binding experiments, EF diluted in HBS-N Buffer at concentration of 50 µl ml^{-1} was injected for 120 sec at a flow rate of 10 µl min^{-1}. BSA diluted 10 µl ml^{-1} was used as control. Regeneration of the matrix was obtained by a short pulse of 10 mM NaOH. SPR experiments were performed in collaboration with Barbara Lelli and Luisa Bracci, Dipartimento di Biologia molecolare, Università degli Studi di Siena, Italy.

Cloning, expression and purification of chimeric proteins

EGFP and mCherry fragments were digested from pRSET A (Invitrogen) with SacI and BstBI and inserted in pRSET A plasmids containing the fragments LF_N or EF_N, respectively, cloned downstream from a N-terminal 6XHis tag coding region, between the restriction sites BamHI and SacI. The coding sequences for EF and LF catalytic regions were PCR-amplified from full length EF and LF in pRSET A, using the following primers: forward 5'- TTT GAG CTC GTG GAA AAA GAT AGG ATT GAT -3' and reverse 5'- AAA GAG CTC TTT TTC ATC AAT AAT TTT TTG GAA G -3' for EF catalytic region; forward 5'- AAA GAG CTC ATG CTG TCA AGA TAT GAA AAA TG -3' and reverse 5'- AAA GAG CTC TGA GTT AAT AAT GAA CTT AAT CT -3' for LF catalytic region. The catalytic EF and LF fragments were digested with SacI and inserted in the construct, downstream LF_N and EF_N, and upstream EGFP and mCherry, respectively. The sequences were confirmed by DNA sequencing. LF_NEF-EGFP and EF_NLF-mCherry were expressed in *Escherichia coli* BL21(DE3)pLysS, grown at 37°C in LB broth containing 100 mg ml^{-1} ampicillin or 100 mg ml^{-1} ampicillin and 34 mg ml^{-1} chloramphenicol. After 4 h of induction with 1 mM isopropyl-1-thio-a-D-galactopyranoside (IPTG) at 30°C, the pellet was resuspended in buffer A (50 mM $Na2HPO_4$, 500 mM NaCl, pH 8) and lysozyme (0.1 mg ml^{-1}). Bacterial cells were disrupted by ultrasonic dispersion and centrifuged, and the supernatant was loaded onto a Hi-trap column charged with Cu_2SO_4 and equilibrated with buffer A. The column was washed with buffer A, the protein was eluted with a 0–100 mM imidazole gradient, the fractions containing chimeric proteins were pooled and dialysed with binding buffer (50 mM Tris, 20 mM NaCl and 1 mM EDTA, pH 7.5) to remove imidazole and NaCl; the yeld was extimated to be ~5 mg L^{-1}. The identities of chimeric proteins were assessed by immunoblotting with anti-6xHis antibodies.

In vitro proteolysis of MKK6

GST- N-terminally fused MKK6 (GST-MKK6) was previously expressed in *E. coli* and affinity- purified on GSH-Sepharose beds. LF or EF_NEF-mCherry were incubated with GST-MKK6 at 37°C for 3 hours in saline buffer (10 mM Tris, 50 mM NaCl, pH 7.5), enzyme:substrate 1:5 ratio. The reactions were

separated by SDS-PAGE and the gel was stained with Comassie Blue.

Conclusions

Anthrax toxins are the major virulence factor secreted by *Bacillus anthracis* during infection. They are delivered to the cell cytoplasm of a great variety of cell types, where they alter crucial signaling pathways through their enzymatic intracellular activity. The understanding of anthrax toxin intracellular trafficking is fundamental to reach a better knowledge of the toxin mode of action and it may also clarify important aspects involved in vesicular trafficking in eukaryotic cells.

In this study we analyze EF and LF intracellular trafficking in single cell using an experimental approach that simulates the conditions found *in vivo* during infection. Chimeric fluorescent EF and LF were video-imaged to localize the two anthrax toxins within live cells, whose physiology is not altered.

Here we show that C-terminally EGFP fused EF and LF are a good tool to report anthrax toxin intracellular trafficking process. They are able to bind $(PA_{63})_7$ on the cell surface, enter the cell, translocate across the $(PA_{63})_7$ pore, and result in cytoplasmic delivery, as they both were active in BHK cell cytoplasm. Conversely, this is not the case for mCherry derivatives, which are not active in cultured cells and do not translocate *in vitro* across $(PA_{63})_7$ channels reconstituted on planar lipid bilayers. We show that mCherry is more resistant to unfolding than EGFP, leading to the knowledge that, when fused to mCherry, EF and LF are not able to unfold and translocate across $(PA_{63})_7$.

Upon rapid endocytosis, EF-EGFP and LF-EGFP were efficiently sorted to a pool of early endosomes containing PI3P and Rab5 but not containing EEA1 or transferrin. The two toxins reach late endosomal compartments enriched in LBPA and localized in the perinuclear area of target cells. Our data is consistent with the kinetics reported for LF and EF activity on cellular substrates [79, 80], supporting the model that indicate late endosomes as the site of anthrax toxin cytoplasmic delivery.

Bibliography

1. Collier, R.J., *Membrane translocation by anthrax toxin.* Mol Aspects Med, 2009. **30**(6): p. 413-22.
2. Pannifer, A.D., et al., *Crystal structure of the anthrax lethal factor.* Nature, 2001. **414**(6860): p. 229-33.
3. Petosa, C., et al., *Crystal structure of the anthrax toxin protective antigen.* Nature, 1997. **385**(6619): p. 833-8.
4. Shen, Y., et al., *Calcium-independent calmodulin binding and two-metal-ion catalytic mechanism of anthrax edema factor.* EMBO J, 2005. **24**(5): p. 929-41.
5. Puhar, A. and C. Montecucco, *Where and how do anthrax toxins exit endosomes to intoxicate host cells?* Trends Microbiol, 2007. **15**(11): p. 477-82.
6. Gruenberg, J. and F.G. van der Goot, *Mechanisms of pathogen entry through the endosomal compartments.* Nat Rev Mol Cell Biol, 2006. **7**(7): p. 495-504.
7. Raiborg, C. and H. Stenmark, *The ESCRT machinery in endosomal sorting of ubiquitylated membrane proteins.* Nature, 2009. **458**(7237): p. 445-52.
8. Schwartz, M., *Dr. Jekyll and Mr. Hyde: a short history of anthrax.* Mol Aspects Med, 2009. **30**(6): p. 347-55.
9. Mock, M. and A. Fouet, *Anthrax.* Annu Rev Microbiol, 2001. **55**: p. 647-71.
10. Turnbull, P.C., *Introduction: anthrax history, disease and ecology.* Curr Top Microbiol Immunol, 2002. **271**: p. 1-19.
11. Koehler, T.M., *Bacillus anthracis physiology and genetics.* Mol Aspects Med, 2009. **30**(6): p. 386-96.
12. Drysdale, M., et al., *atxA controls Bacillus anthracis capsule synthesis via acpA and a newly discovered regulator, acpB.* J Bacteriol, 2004. **186**(2): p. 307-15.
13. Smith, H., J. Keppie, and J.L. Stanley, *The chemical basis of the virulence of Bacillus anthracis. V. The specific toxin produced by B. Anthracis in vivo.* Br J Exp Pathol, 1955. **36**(5): p. 460-72.
14. Hudson, M.J., et al., *Bacillus anthracis: balancing innocent research with dual-use potential.* Int J Med Microbiol, 2008. **298**(5-6): p. 345-64.
15. Tournier, J.N., et al., *Anthrax toxins: a weapon to systematically dismantle the host immune defenses.* Mol Aspects Med, 2009. **30**(6): p. 456-66.
16. Ascenzi, P., et al., *Anthrax toxin: a tripartite lethal combination.* FEBS Lett, 2002. **531**(3): p. 384-8.
17. Lacy, D.B., et al., *Structure of heptameric protective antigen bound to an anthrax toxin receptor: a role for receptor in pH-dependent pore formation.* Proc Natl Acad Sci U S A, 2004. **101**(36): p. 13147-51.
18. Wesche, J., et al., *Characterization of membrane translocation by anthrax protective antigen.* Biochemistry, 1998. **37**(45): p. 15737-46.
19. Zhang, S., A. Finkelstein, and R.J. Collier, *Evidence that translocation of anthrax toxin's lethal factor is initiated by entry of its N terminus into the protective antigen channel.* Proc Natl Acad Sci U S A, 2004. **101**(48): p. 16756-61.
20. Liang, X., et al., *Involvement of domain II in toxicity of anthrax lethal factor.* J Biol Chem, 2004. **279**(50): p. 52473-8.
21. Tonello, F. and C. Montecucco, *The anthrax lethal factor and its MAPK kinase-specific metalloprotease activity.* Mol Aspects Med, 2009. **30**(6): p. 431-8.
22. Drum, C.L., et al., *Structural basis for the activation of anthrax adenylyl cyclase exotoxin by calmodulin.* Nature, 2002. **415**(6870): p. 396-402.
23. Shen, Y., et al., *Physiological calcium concentrations regulate calmodulin binding and catalysis of adenylyl cyclase exotoxins.* EMBO J, 2002. **21**(24): p. 6721-32.
24. Bradley, K.A., et al., *Identification of the cellular receptor for anthrax toxin.* Nature, 2001. **414**(6860): p. 225-9.
25. Scobie, H.M., et al., *Human capillary morphogenesis protein 2 functions as an anthrax toxin receptor.* Proc Natl Acad Sci U S A, 2003. **100**(9): p. 5170-4.
26. Scobie, H.M. and J.A. Young, *Interactions between anthrax toxin receptors and protective antigen.* Curr Opin Microbiol, 2005. **8**(1): p. 106-12.
27. Bradley, K.A., et al., *Binding of anthrax toxin to its receptor is similar to alpha integrin-ligand interactions.* J Biol Chem, 2003. **278**(49): p. 49342-7.

28. Wigelsworth, D.J., et al., *Binding stoichiometry and kinetics of the interaction of a human anthrax toxin receptor, CMG2, with protective antigen.* J Biol Chem, 2004. **279**(22): p. 23349-56.
29. Go, M.Y., E.M. Chow, and J. Mogridge, *The cytoplasmic domain of anthrax toxin receptor 1 affects binding of the protective antigen.* Infect Immun, 2009. **77**(1): p. 52-9.
30. Abrami, L., S.H. Leppla, and F.G. van der Goot, *Receptor palmitoylation and ubiquitination regulate anthrax toxin endocytosis.* J Cell Biol, 2006. **172**(2): p. 309-20.
31. Bonuccelli, G., et al., *ATR/TEM8 is highly expressed in epithelial cells lining Bacillus anthracis' three sites of entry: implications for the pathogenesis of anthrax infection.* Am J Physiol Cell Physiol, 2005. **288**(6): p. C1402-10.
32. Maldonado-Arocho, F.J., et al., *Anthrax oedema toxin induces anthrax toxin receptor expression in monocyte-derived cells.* Mol Microbiol, 2006. **61**(2): p. 324-37.
33. Xu, Q., E.D. Hesek, and M. Zeng, *Transcriptional stimulation of anthrax toxin receptors by anthrax edema toxin and Bacillus anthracis Sterne spore.* Microb Pathog, 2007. **43**(1): p. 37-45.
34. Molloy, S.S., et al., *Human furin is a calcium-dependent serine endoprotease that recognizes the sequence Arg-X-X-Arg and efficiently cleaves anthrax toxin protective antigen.* J Biol Chem, 1992. **267**(23): p. 16396-402.
35. Milne, J.C., et al., *Anthrax protective antigen forms oligomers during intoxication of mammalian cells.* J Biol Chem, 1994. **269**(32): p. 20607-12.
36. Mogridge, J., et al., *The lethal and edema factors of anthrax toxin bind only to oligomeric forms of the protective antigen.* Proc Natl Acad Sci U S A, 2002. **99**(10): p. 7045-8.
37. Lacy, D.B., et al., *Mapping the anthrax protective antigen binding site on the lethal and edema factors.* J Biol Chem, 2002. **277**(4): p. 3006-10.
38. Bragg, T.S. and D.L. Robertson, *Nucleotide sequence and analysis of the lethal factor gene (lef) from Bacillus anthracis.* Gene, 1989. **81**(1): p. 45-54.
39. Arora, N., et al., *Fusions of anthrax toxin lethal factor to the ADP-ribosylation domain of Pseudomonas exotoxin A are potent cytotoxins which are translocated to the cytosol of mammalian cells.* J Biol Chem, 1992. **267**(22): p. 15542-8.
40. Cunningham, K., et al., *Mapping the lethal factor and edema factor binding sites on oligomeric anthrax protective antigen.* Proc Natl Acad Sci U S A, 2002. **99**(10): p. 7049-53.
41. Mogridge, J., K. Cunningham, and R.J. Collier, *Stoichiometry of anthrax toxin complexes.* Biochemistry, 2002. **41**(3): p. 1079-82.
42. Blaustein, R.O., et al., *Anthrax toxin: channel-forming activity of protective antigen in planar phospholipid bilayers.* Proc Natl Acad Sci U S A, 1989. **86**(7): p. 2209-13.
43. Milne, J.C. and R.J. Collier, *pH-dependent permeabilization of the plasma membrane of mammalian cells by anthrax protective antigen.* Mol Microbiol, 1993. **10**(3): p. 647-53.
44. Benson, E.L., et al., *Identification of residues lining the anthrax protective antigen channel.* Biochemistry, 1998. **37**(11): p. 3941-8.
45. Katayama, H., et al., *GroEL as a molecular scaffold for structural analysis of the anthrax toxin pore.* Nat Struct Mol Biol, 2008. **15**(7): p. 754-60.
46. Krantz, B.A., et al., *Acid-induced unfolding of the amino-terminal domains of the lethal and edema factors of anthrax toxin.* J Mol Biol, 2004. **344**(3): p. 739-56.
47. Krantz, B.A., et al., *A phenylalanine clamp catalyzes protein translocation through the anthrax toxin pore.* Science, 2005. **309**(5735): p. 777-81.
48. Young, J.A. and R.J. Collier, *Anthrax toxin: receptor binding, internalization, pore formation, and translocation.* Annu Rev Biochem, 2007. **76**: p. 243-65.
49. Neumeyer, T., et al., *Anthrax edema factor, voltage-dependent binding to the protective antigen ion channel and comparison to LF binding.* J Biol Chem, 2006. **281**(43): p. 32335-43.
50. Melnyk, R.A. and R.J. Collier, *A loop network within the anthrax toxin pore positions the phenylalanine clamp in an active conformation.* Proc Natl Acad Sci U S A, 2006. **103**(26): p. 9802-7.
51. Arora, N. and S.H. Leppla, *Residues 1-254 of anthrax toxin lethal factor are sufficient to cause cellular uptake of fused polypeptides.* J Biol Chem, 1993. **268**(5): p. 3334-41.
52. Arora, N. and S.H. Leppla, *Fusions of anthrax toxin lethal factor with shiga toxin and diphtheria toxin enzymatic domains are toxic to mammalian cells.* Infect Immun, 1994. **62**(11): p. 4955-61.
53. Gupta, P.K., et al., *Role of N-terminal amino acids in the potency of anthrax lethal factor.* PLoS One, 2008. **3**(9): p. e3130.
54. Wickliffe, K.E., S.H. Leppla, and M. Moayeri, *Killing of macrophages by anthrax lethal toxin: involvement of the N-end rule pathway.* Cell Microbiol, 2008. **10**(6): p. 1352-62.
55. Rink, J., et al., *Rab conversion as a mechanism of progression from early to late endosomes.* Cell, 2005. **122**(5): p. 735-49.
56. Kutateladze, T.G., *Translation of the phosphoinositide code by PI effectors.* Nat Chem Biol, 2010. **6**(7): p. 507-13.
57. Gruenberg, J., *The endocytic pathway: a mosaic of domains.* Nat Rev Mol Cell Biol, 2001. **2**(10): p. 721-730.
58. Woodman, P.G. and C.E. Futter, *Multivesicular bodies: co-ordinated progression to maturity.* Curr Opin Cell Biol, 2008. **20**(4): p. 408-14.

59. Gillooly, D.J., et al., *Localization of phosphatidylinositol 3-phosphate in yeast and mammalian cells.* EMBO J, 2000. **19**(17): p. 4577-88.
60. Sorkin, A. and M. von Zastrow, *Endocytosis and signalling: intertwining molecular networks.* Nat Rev Mol Cell Biol, 2009. **10**(9): p. 609-22.
61. Katzmann, D.J., G. Odorizzi, and S.D. Emr, *Receptor downregulation and multivesicular-body sorting.* Nat Rev Mol Cell Biol, 2002. **3**(12): p. 893-905.
62. Simonsen, A., et al., *The role of phosphoinositides in membrane transport.* Curr Opin Cell Biol, 2001. **13**(4): p. 485-92.
63. Bache, K.G., et al., *Hrs regulates multivesicular body formation via ESCRT recruitment to endosomes.* J Cell Biol, 2003. **162**(3): p. 435-42.
64. Hurley, J.H. and S.D. Emr, *The ESCRT complexes: structure and mechanism of a membrane-trafficking network.* Annu Rev Biophys Biomol Struct, 2006. **35**: p. 277-98.
65. Falguieres, T., et al., *In vitro budding of intralumenal vesicles into late endosomes is regulated by Alix and Tsg101.* Mol Biol Cell, 2008. **19**(11): p. 4942-55.
66. Hurley, J.H., *ESCRT complexes and the biogenesis of multivesicular bodies.* Curr Opin Cell Biol, 2008. **20**(1): p. 4-11.
67. Kobayashi, T., et al., *A lipid associated with the antiphospholipid syndrome regulates endosome structure and function.* Nature, 1998. **392**(6672): p. 193-7.
68. Griffiths, G., et al., *The mannose 6-phosphate receptor and the biogenesis of lysosomes.* Cell, 1988. **52**(3): p. 329-41.
69. Kobayashi, T., et al., *Late endosomal membranes rich in lysobisphosphatidic acid regulate cholesterol transport.* Nat Cell Biol, 1999. **1**(2): p. 113-8.
70. Luyet, P.P., et al., *The ESCRT-I subunit TSG101 controls endosome-to-cytosol release of viral RNA.* Traffic, 2008. **9**(12): p. 2279-90.
71. Falguieres, T., P.P. Luyet, and J. Gruenberg, *Molecular assemblies and membrane domains in multivesicular endosome dynamics.* Exp Cell Res, 2009. **315**(9): p. 1567-73.
72. Kobayashi, T., et al., *Separation and characterization of late endosomal membrane domains.* J Biol Chem, 2002. **277**(35): p. 32157-64.
73. Bright, N.A., M.J. Gratian, and J.P. Luzio, *Endocytic delivery to lysosomes mediated by concurrent fusion and kissing events in living cells.* Curr Biol, 2005. **15**(4): p. 360-5.
74. Luzio, J., P. Pryor, and N. Bright, *Lysosomes: fusion and function.* Nature Reviews Molecular Cell Biology, 2007. **8**(8): p. 622-632.
75. Abrami, L., et al., *Anthrax toxin triggers endocytosis of its receptor via a lipid raft-mediated clathrin-dependent process.* J Cell Biol, 2003. **160**(3): p. 321-8.
76. Beauregard, K.E., R.J. Collier, and J.A. Swanson, *Proteolytic activation of receptor-bound anthrax protective antigen on macrophages promotes its internalization.* Cell Microbiol, 2000. **2**(3): p. 251-8.
77. Boll, W., et al., *Effects of dynamin inactivation on pathways of anthrax toxin uptake.* Eur J Cell Biol, 2004. **83**(6): p. 281-8.
78. Zornetta, I., et al., *Imaging the cell entry of the anthrax oedema and lethal toxins with fluorescent protein chimeras.* Cell Microbiol, 2010. **12**(10): p. 1435-45.
79. Abrami, L., et al., *Membrane insertion of anthrax protective antigen and cytoplasmic delivery of lethal factor occur at different stages of the endocytic pathway.* J Cell Biol, 2004. **166**(5): p. 645-51.
80. Dal Molin, F., et al., *Cell entry and cAMP imaging of anthrax edema toxin.* EMBO J, 2006. **25**(22): p. 5405-13.
81. Guidi-Rontani, C., et al., *Translocation of Bacillus anthracis lethal and oedema factors across endosome membranes.* Cell Microbiol, 2000. **2**(3): p. 259-64.
82. Le Blanc, I., et al., *Endosome-to-cytosol transport of viral nucleocapsids.* Nature cell biology, 2005. **7**(7): p. 653-664.
83. Wang, X.M., et al., *Structure and interaction of PA63 and EF (edema toxin) of Bacillus anthracis with lipid membrane.* Biochemistry, 1997. **36**(48): p. 14906-13.
84. Keppie, J., H. Smith, and P.W. Harris-Smith, *The chemical basis of the virulence of Bacillus anthracis. III. The role of the terminal bacteraemia in death of guinea-pigs from anthrax.* Br J Exp Pathol, 1955. **36**(3): p. 315-22.
85. Chang, L. and M. Karin, *Mammalian MAP kinase signalling cascades.* Nature, 2001. **410**(6824): p. 37-40.
86. Pearson, G., et al., *Mitogen-activated protein (MAP) kinase pathways: regulation and physiological functions.* Endocr Rev, 2001. **22**(2): p. 153-83.
87. Turk, B.E., *Manipulation of host signalling pathways by anthrax toxins.* Biochem J, 2007. **402**(3): p. 405-17.
88. Chopra, A.P., et al., *Anthrax lethal factor proteolysis and inactivation of MAPK kinase.* J Biol Chem, 2003. **278**(11): p. 9402-6.
89. Gonzalez-Gaitan, M., *Signal dispersal and transduction through the endocytic pathway.* Nat Rev Mol Cell Biol, 2003. **4**(3): p. 213-24.
90. Tang, W.J. and J.H. Hurley, *Catalytic mechanism and regulation of mammalian adenylyl cyclases.* Mol Pharmacol, 1998. **54**(2): p. 231-40.

91. Matsumoto, G., *Bioterrorism. Anthrax powder: state of the art?* Science, 2003. **302**(5650): p. 1492-7.
92. Kim, C., et al., *Antiinflammatory cAMP signaling and cell migration genes co-opted by the anthrax bacillus.* Proc Natl Acad Sci U S A, 2008. **105**(16): p. 6150-5.
93. Rossi Paccani, S., et al., *Anthrax toxins inhibit immune cell chemotaxis by perturbing chemokine receptor signalling.* Cell Microbiol, 2007. **9**(4): p. 924-9.
94. Friedlander, A.M., et al., *Characterization of macrophage sensitivity and resistance to anthrax lethal toxin.* Infect Immun, 1993. **61**(1): p. 245-52.
95. Boyden, E.D. and W.F. Dietrich, *Nalp1b controls mouse macrophage susceptibility to anthrax lethal toxin.* Nat Genet, 2006. **38**(2): p. 240-4.
96. Park, J.M., et al., *Signaling pathways and genes that inhibit pathogen-induced macrophage apoptosis--CREB and NF-kappaB as key regulators.* Immunity, 2005. **23**(3): p. 319-29.
97. Alileche, A., et al., *Anthrax lethal toxin-mediated killing of human and murine dendritic cells impairs the adaptive immune response.* PLoS Pathog, 2005. **1**(2): p. e19.
98. Agrawal, A., et al., *Impairment of dendritic cells and adaptive immunity by anthrax lethal toxin.* Nature, 2003. **424**(6946): p. 329-34.
99. Tournier, J.N., et al., *Anthrax edema toxin cooperates with lethal toxin to impair cytokine secretion during infection of dendritic cells.* J Immunol, 2005. **174**(8): p. 4934-41.
100. Fang, H., et al., *Anthrax lethal toxin has direct and potent inhibitory effects on B cell proliferation and immunoglobulin production.* J Immunol, 2006. **176**(10): p. 6155-61.
101. Moayeri, M. and S.H. Leppla, *Cellular and systemic effects of anthrax lethal toxin and edema toxin.* Mol Aspects Med, 2009. **30**(6): p. 439-55.
102. Liu, S., et al., *Matrix metalloproteinase-activated anthrax lethal toxin demonstrates high potency in targeting tumor vasculature.* J Biol Chem, 2008. **283**(1): p. 529-40.
103. Bolcome, R.E., 3rd, et al., *Anthrax lethal toxin induces cell death-independent permeability in zebrafish vasculature.* Proc Natl Acad Sci U S A, 2008. **105**(7): p. 2439-44.
104. Warfel, J.M., A.D. Steele, and F. D'Agnillo, *Anthrax lethal toxin induces endothelial barrier dysfunction.* Am J Pathol, 2005. **166**(6): p. 1871-81.
105. Lehmann, M., et al., *Lung epithelial injury by B. anthracis lethal toxin is caused by MKK-dependent loss of cytoskeletal integrity.* PLoS One, 2009. **4**(3): p. e4755.
106. Molin, F.D., et al., *Ratio of lethal and edema factors in rabbit systemic anthrax.* Toxicon, 2008. **52**(7): p. 824-8.
107. Sirard, J.C., M. Mock, and A. Fouet, *The three Bacillus anthracis toxin genes are coordinately regulated by bicarbonate and temperature.* J Bacteriol, 1994. **176**(16): p. 5188-92.
108. Shaner, N.C., P.A. Steinbach, and R.Y. Tsien, *A guide to choosing fluorescent proteins.* Nat Methods, 2005. **2**(12): p. 905-9.
109. Abrami, L., B. Kunz, and F.G. van der Goot, *Anthrax toxin triggers the activation of src-like kinases to mediate its own uptake.* Proc Natl Acad Sci U S A, 2010. **107**(4): p. 1420-4.
110. Teis, D., W. Wunderlich, and L.A. Huber, *Localization of the MP1-MAPK scaffold complex to endosomes is mediated by p14 and required for signal transduction.* Dev Cell, 2002. **3**(6): p. 803-14.
111. Park, J.M., et al., *Macrophage apoptosis by anthrax lethal factor through p38 MAP kinase inhibition.* Science, 2002. **297**(5589): p. 2048-51.
112. Zaccolo, M. and T. Pozzan, *Discrete microdomains with high concentration of cAMP in stimulated rat neonatal cardiac myocytes.* Science, 2002. **295**(5560): p. 1711-5.
113. Kimura, R.H., E.R. Steenblock, and J.A. Camarero, *Development of a cell-based fluorescence resonance energy transfer reporter for Bacillus anthracis lethal factor protease.* Anal Biochem, 2007. **369**(1): p. 60-70.
114. Vitale, G., et al., *Susceptibility of mitogen-activated protein kinase kinase family members to proteolysis by anthrax lethal factor.* Biochem J, 2000. **352 Pt 3**: p. 739-45.
115. Lissandron, V., et al., *Improvement of a FRET-based indicator for cAMP by linker design and stabilization of donor-acceptor interaction.* J Mol Biol, 2005. **354**(3): p. 546-55.
116. Mongillo, M., et al., *Study of cyclic adenosine monophosphate microdomains in cells.* Methods Mol Biol, 2005. **307**: p. 1-13.
117. Janowiak, B.E., A. Finkelstein, and R.J. Collier, *An approach to characterizing single-subunit mutations in multimeric prepores and pores of anthrax protective antigen.* Protein Sci, 2009. **18**(2): p. 348-58.

Acknowledgments

The present study was carried out at the Department of Sperimental Biomedical Sciences, Università di Padova. It is my pleasure to thank Prof. Cesare Montecucco and Dott.ssa Fiorella Tonello for giving me the opportunity to perform this doctoral thesis. Special thanks go to Dott.ssa Irene Zornetta and Dott.ssa Federica dal Molin who have collaborated giving their effort and support to this work. Thanks also to Dott.ssa Barbara Lelli for introducing me to SPR and for the stimulating suggestions. Furthermore, I would like to thank all the members of Prof. van der Goot laboratory for their consistent support. Project funding was by Cariparo.